

Effect of pre-strain and pre-corrosion on ratcheting behavior of ASTM A668 Class D steel

Subhrasmita Tripathy



Department of Metallurgical and Materials
Engineering
National Institute of Technology Rourkela

Effect of pre-strain and pre-corrosion on ratcheting behavior of ASTM A668 Class D steel

*Dissertation submitted to the
National Institute of Technology Rourkela*

*In partial fulfillment of the
requirements of the degree of
Master of Technology (By research)*

*in
Metallurgical and Materials Engineering*

*by
Subhrasmita Tripathy*

(Roll Number: 612MM2007)

under the supervision of

Prof. Krishna Dutta

and

Prof. Ashok Kumar Mondal



January, 2016

Department of Metallurgical and Materials Engineering
National Institute of Technology Rourkela



Metallurgical and Materials Engineering
National Institute of Technology Rourkela

October 3, 2016

Certificate of Examination

Roll Number: 612MM1007

Name: Subhrasmita Tripathy

Title of Dissertation: Effect of pre-strain and pre-corrosion on ratcheting behavior of ASTM A668 Class D steel

We the below signed, after checking the dissertation mentioned above and the official record book(s) of the student, hereby state our approval of the dissertation submitted in partial fulfillment of the requirements of the degree of Master of Technology (Research) in Metallurgical and Materials Engineering at National Institute of Technology Rourkela. We are satisfied with the volume, quality, correctness, and originality of the work.

<Ashok Kumar Mondal>
Co-Supervisor

< Krishna Dutta >
Principal Supervisor

< Debasis Chaira >
Member (MSC)

< Shantanu Paria >
Member (MSC)

< A. Thirugnanam >
Member (MSC)

Examiner

< Subash Chandra Mishra >
Chairman (MSC)



Metallurgical and Materials Engineering
National Institute of Technology Rourkela

October 3, 2016

Supervisor's Certificate

This is to certify that the work presented in this dissertation entitled "*Effect of pre-strain and pre-corrosion on ratcheting behavior of ASTM A668 Class D steel*" by "*Subhrasmita Tripathy*", Roll Number 612MM1007, are in record of original research carried out by her under our supervision and guidance in partial fulfillment of the requirements of the degree of *Master of Technology (Research)* in *Metallurgical and Materials Engineering*. Neither this dissertation nor any part of it has been submitted for any degree or diploma to any institute or university in India or abroad.

Ashok Kumar Mondal

Co-Supervisor

Krishna Dutta

Principal Supervisor

Dedication

There are a number of people without whom this thesis might not have been written, and to whom I am greatly indebted.

To my parents, Sanjay and Sneha Tripathy whose words of encouragement and push for tenacity ring in my ears. A special thanks to my mother Sneha who has been a source of encouragement and inspiration to me throughout my life. And also for the myriad of ways in which, throughout my life, you have actively supported me in my determination to find and realize my potential.

Declaration of Originality

I, Subhrasmita Tripathy, Roll Number 612MM1007 hereby declare that this dissertation entitled "*Effect of pre-strain and pre-corrosion on ratcheting behavior of A668 Class D steel*" represents my original work carried out as a postgraduate student of NIT Rourkela and, to the best of my knowledge, it contains no material previously published or written by another person, nor any material presented for the award of any other degree or diploma of NIT Rourkela or any other institution. Any contribution made to this research by others, with whom I have worked at NIT Rourkela or elsewhere, is explicitly acknowledged in the dissertation. Works of other authors cited in this dissertation have been duly acknowledged under the section "Bibliography". I have also submitted my original research records to the scrutiny committee for evaluation of my dissertation.

I am fully aware that in case of any non compliance detected in future, the Senate of NIT Rourkela may withdraw the degree awarded to me on the basis of the present dissertation.

January 15, 2016
NIT Rourkela

Subhrasmita Tripathy

Acknowledgment

A journey is easier when you travel together. This thesis is the results of years of work whereby I have been guided and supported by many people. Hence, this would be worthwhile and pleasing to express sense of gratitude for all of them.

I would like to express my deep sense of gratitude to my supervisors **Prof. Krishna Dutta** and **Prof. A.K. Mondal** Assistant Professor, NIT, Rourkela for their invaluable guidance, motivation, untiring efforts, meticulous attention and support throughout my research work. It would have not been possible for me to bring out this thesis without their help and constant encouragement.

I am sincerely thankful to **Prof. S.C. Mishra**, Professor and Head Metallurgical and Materials Engineering Department and other faculty members of this department for their persistent support and advice during the course work.

I am also highly grateful to laboratory members of Department of Metallurgical and Materials Engineering, NIT Rourkela, specially Mr. Hembram, Mr. R. Pattanaik, Mr. S. Pradhan and Mr. A. Pal for their help during the execution of experiments.

Finally, I feel great reverence for all my family members and the Almighty, for their blessings and for being a constant source of encouragement.

January 15, 2016
NIT Rourkela

Subhrasmita Tripathy
Roll Number: 612MM1007

Abstract

Ratcheting can be considered as one of the serious problems as this phenomenon causes premature failure of structural components. Ratcheting deformation can be regarded as the stress controlled low cycle fatigue (LCF) response of a material which occurs due to accumulation of plastic strain during asymmetric cyclic loading. Ratcheting is dependant on various parameters like material chemistry, stress states and environmental issues. The aim of this investigation was to study the effect of pre-strain (0%, 2%, 4% and 8%) on ratcheting in different heat treated conditions (normalized and hardened-tempered). The effect of pre-corrosion (7, 14 and 21 days in 3.5% NaCl solution) on the nature and extent of strain accumulation was also studied. Ratcheting tests were carried out at room temperature on cylindrical specimens having 12.5 mm gauge length and 6 mm gauge diameter. The results include reduced strain accumulation with increasing pre-strain strain level due to work hardening of the pre-strained samples. Further cyclic hardening takes place during ratcheting deformation. Pre-corroded samples showed more amount of strain accumulation compared to the samples without corrosion. Post ratcheting tensile strength increases in all the tested samples owing to cyclic hardening during ratcheting. The factographic studies indicated typical dimple features.

Keywords: Ratcheting; Pre-strain; Hardening behavior; Pre-Corrosion

Contents

Certificate of Examination	iii
Supervisors' Certificate	iv
Dedication	v
Declaration of Originality	vi
Acknowledgment	vii
Abstract	viii
List of Figures	ix
List of Tables	ix
1 Introduction	1
1.1 Introduction.....	1
1.2 Organization of the thesis.....	2
2 Literature review	3
2.1 Fatigue.....	3
2.2 Types of load applications.....	4
2.3 Types of fatigue.....	6
2.3.1 Low cycle fatigue.....	6
2.3.2 High cycle fatigue.....	7
2.4 Effect of mean stress on fatigue.....	7
2.5 Ratcheting.....	10
2.6 Factors affecting ratcheting.....	12
2.6.1 Pre-strain.....	12
2.6.2 Corrosion-Fatigue.....	13

2.7	Reappraisal of the current problem.....	14
3	Experimental Procedures	15
3.1	Material selection and chemical composition.....	16
3.2	Heat treatment.....	15
3.2.1	Normalizing.....	15
3.2.2	Hardening and tempering.....	15
3.3	Microstructural characterization.....	15
3.4	Mechanical testing.....	16
3.4.1	Hardness testing.....	16
3.4.2	Tensile testing.....	16
3.5	Ratcheting study.....	17
3.6	Corrosion fatigue test.....	19
3.7	Post ratcheting tensile test.....	19
4	Results and discussion	22
4.1	Microstructural analysis.....	22
4.2	Hardness.....	24
4.3	Tensile behavior.....	24
4.4	Ratcheting behavior.....	28
4.4.1	Effect of pre-strain on ratcheting of normalized steel.....	28
4.4.2	Effect of pre-strain on ratcheting of hardened tempered steel.....	30
4.4.3	Saturation in strain accumulation.....	33
4.4.4	Ratcheting test on pre-corroded samples.....	35
4.6	Post tensile ratcheting	40
4.7	Fractographic observation.....	42
5	Conclusion	45
	Bibliography	48
	Dissemination	53
	Vitae	54

List of Figures

2.1	Schematic representation of various stages of fatigue life of a component.	5
2.2	Types of loading imposed on a component (a) symmetric loading (b) asymmetric loading and (c) irregular loading.	5
2.3	Graphical representation of Coffin-Manson relationship.	8
2.4	Plot of cyclic hardening/softening behavior in low cycle fatigue.	8
2.5	Effect of mean stress on endurance limit.	9
2.6	Schematic representation of ratcheting phenomenon.	11
3.1	Sample design for tensile test.	18
3.2	Sample design for fatigue test.	18
3.3	Schematic diagram representing the corrosion bath.	20
3.4	Photograph of a broken post ratcheting tensile sample.	21
4.1	Optical microstructures of the steel in normalized and hardened-tempered condition.	23
4.2	Engineering stress-strain curves of normalized and hardened-tempered samples of the investigated steel.	26
4.3	Typical $\log(\sigma) - \log(\epsilon)$ plots for normalized and hardened-tempered samples of ASTM A668 Class D Steel.	27

4.4	(a) Effect of pre-strain on accumulation of ratcheting strain and (b) hysteresis loops produced during ratcheting in normalized steel.	29
4.5	(a) Effect of pre-strain on accumulation of ratcheting strain and (b) hysteresis loops produced during ratcheting in hardened-tempered steel.	32
4.6	Variations in the rate of accumulation of ratcheting strain with increasing number of cycles for (a) normalized and (b) hardened-tempered A668 class D steel at different levels of pre-strain.	34
4.7	Photographs of corroded samples of (a) 7 days (b) 14 days (c) 21 days.	36
4.8	Histograms representing accumulation of ratcheting strain on corroded samples from 7 to 21 days at (a) 0% (b) 2% (c) 4% and (d) 8% pre-strain.	38
4.9	Ratcheting behavior of pre-corroded samples for (a) 7 days (b) 14 days (c) 21 days with pre-strain.	40
4.10	Post ratcheting tensile stress-strain plots of (a) normalized and (b) hardened-tempered samples of investigated steel.	42
4.11	Fracture surfaces of broken post-ratcheting tensile specimens with EDS spectra obtained from the inclusions present in the specimens corresponding to normalized and pre-strain levels of (a) 2% and (c) 8%.	44
4.12	Typical fractographs obtained from the post-ratcheting broken tensile specimens (hardened-tempered) owing to pre-strain levels of (a) 2% and (b) 8%.	45

List of Tables

3.1	Chemical composition of the investigated ASTM A668 class D steel.	14
4.1	Vickers hardness values of normalized and hardened-tempered samples of the investigated steel.	24
4.2	Tensile properties of investigated steel.	28
4.3	Post ratcheting tensile properties for normalized and hardened-tempered samples at different levels of pre-strain.	41

Chapter 1

Introduction

1.1 Introduction

ASTM A668 class D steel is a plain carbon steel which is potentially being used in various engineering sectors like aerospace, automotive and defense applications. In these kind of applications, the most important property requirements are good fatigue and fracture behavior of the material. It is known that 90% of all service failures are due to fatigue [1] and hence, it is important to know the fatigue behavior of the steel. Traditionally, strain-controlled low cycle or stress-controlled high cycle fatigue studies are being performed to assess the fatigue behavior of a material. However, in recent days researchers are paying much attention towards generating information regarding stress-controlled low cycle fatigue behavior of a material; the phenomenon is known as ratcheting. Ratcheting deformation is much pronounced in the presence of some positive or negative mean stress. Accumulation of ratcheting strain during cyclic loading reduces low cycle fatigue life of a material. Therefore, it is one of the important factors that should be considered in the design of any structural component [2-6]. Accordingly, the ratcheting fatigue behavior of the ASTM A668 Class D steel is investigated in the present thesis.

It is further known that materials undergo degradation when they are exposed to reactive environment. Therefore, cyclic loading of a component under aggressive environment causes additional damage. The materials subjected to combined effect of fatigue and corrosion is known as corrosion-fatigue. Several surveys exhibited reasonably large number of failures occurs due to combined effect of corrosion and fatigue [7]. Experimental studies revealed that cracks due to corrosion fatigue start from the surface pits of a material [8]. The presence of pitting corrosion reported to reduce fatigue life of materials metals used in structural applications. Therefore, it is of immense importance to study the ratcheting behavior of the pre-corroded steel.

1.2 Organization of the thesis

The present thesis is organized as follows:

Chapter 1 gives information about the importance of fatigue-ratcheting studies of the ASTM A668 class D steel. The motivation and overview of the present work are described in this chapter.

Chapter 2 includes review of existing works related to ratcheting and corrosion-fatigue. Effect of pre-strain on ratcheting is discussed.

Chapter 3 presents the detailed information about the experiments conducted in this work.

Chapter 4 includes results and discussion on microstructural analysis, hardness, tensile, fatigue and corrosion tests. Characteristics of fracture surfaces of normalized and hardened-tempered steels after fatigue test are also discussed.

Chapter 5 comprises the summary of the present work. It also provides the directions for further investigation. At the end, the references followed during this investigation are listed.

Chapter 2

Literature Review

In this chapter the summary of literature surveyed during the course of this research work has been presented. This literature survey provides background information and thus to select the objectives of the present investigation.

2.1 Fatigue

When a component is subjected to fluctuating stress, it may fail at stress levels much lower than its monotonic fracture strength. Failures occurring under conditions of dynamic loading are called as fatigue failure. Fatigue has become progressively more relevant in developed technology in the areas, such as automobiles, aircraft, compressors, pumps, turbines, etc. It is a phenomenon associated with the initiation and propagation of cracks to an unstable size. When the crack reaches a critical dimension, one additional cycle causes sudden failure. It is considered that almost 90% of all the service failures occur due to fatigue [1]. Structural components when subjected to repeated cyclic loading and unloading over a long period of time, the nature of their operation usually fails at stress levels significantly lower than their monotonic fracture strength [9-10]. The basic factors that are necessary to cause fatigue failure are given below:

- (i) The maximum tensile stress of sufficiently high values.
- (ii) Large enough variation and fluctuation in the applied stress.
- (iii) A large number of cycles of the stress applied.

As the minute cracks grow during the service life of components, process of fatigue fracture is progressive. In crystalline structure of metals and alloys sub-microscopic changes take place under the action of repetitive low level load applications. These minute changes accumulate to form minute microscopic cracks. These small cracks gradually grows under

cyclic loading and results in formation of larger cracks. When a sudden failure occurs the larger cracks continue to grow until the stress in the remaining ligament becomes indefensible. The three different stages of fatigue are:

- a) Fatigue softening and/or hardening takes place as a result of the interaction involving structural defects mainly dislocations in the completely loaded volume. Basically the parameters of cyclic loading like stress ratio, mean stress, stress amplitude, temperature decides the fatigue hardening and softening of the material.
- b) Initiation of the fatigue cracks during cyclic loading occurs at localized plastic deformation at nucleation sites. Crack propagation is mainly governed by the cyclic plastic deformation confined in the plastic zone.

Fig. 2.1 represents various stages of fatigue process. The three curves of Fig. 2.1 represent the complete fatigue process i.e. end of the softening/hardening stage, end of the crack nucleation stage, the end of fatigue crack propagation stage. The more expected sites for a crack initiation are pre-existing highly stressed areas, pits, scratches, inclusions on the surface and discontinuities along the crystallographic planes. Fatigue crack usually begins when their primary growth is mostly in the direction of the maximum shear stress and there is major internal flaw such as large inclusions at the surface of the specimen.

2.2 Types of load application

Figure 2.2. and fig. 2.2 (a) represents a completely reversed cycle of stress of sinusoidal form. This represents symmetric cyclic loading with mean stress equal to zero. The tensile stress is considered positive, whereas, compressive stress is negative. Figure 2.2 (b) represents an asymmetric cyclic loading. The figure clearly depicts that the value of mean stress is not equal to zero and it shows that both σ_{\max} and σ_{\min} in tension. In asymmetric cyclical loading both the maximum and minimum stress could be of opposite sign or both in tension or compression. Figure 2.2 (c) represents a random cycle where the component might be subjected to periodic, unpredictable loading as in aircraft wings due to gusts.

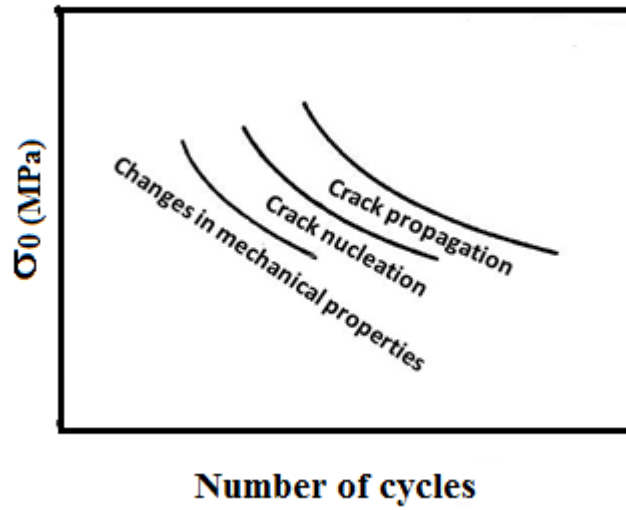


Fig. 2.1: Schematic representation of various stages of fatigue life of a component [1].

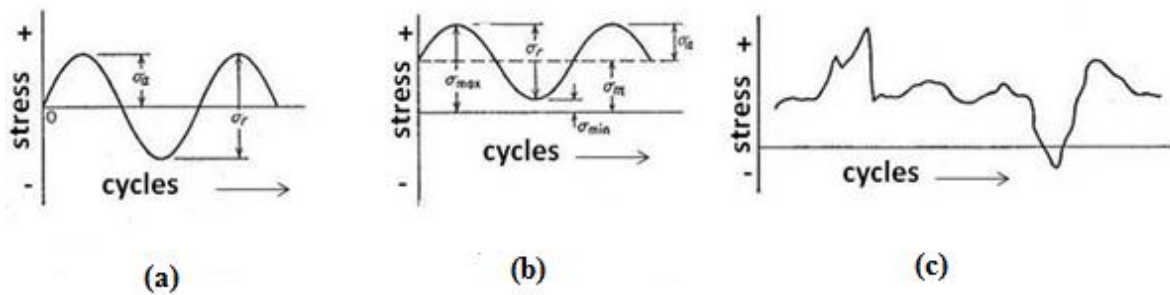


Fig. 2.2: Types of loading imposed on a component (a) symmetric loading (b) asymmetric loading and (c) irregular loading [1].

2.3 Types of fatigue

Fatigue can be broadly divided into two types i.e. high cycle fatigue and low cycle fatigue. High cycle fatigue is the fatigue condition in which the number of cycles to failure is more than 10^5 cycles, and when the number of cycles to failure is less than 10^4 - 10^5 cycles, the fatigue condition is called low cycle fatigue.

2.3.1 Low cycle fatigue

LCF is mainly associated with higher loads (plastic deformation occurs) and shorter life. The corresponding stress level is normally below 2/3 of yielding stress. The stress level usually steps into plastic range. An example of structures where the low cycle fatigue (LCF) can be important part is pressure vessels, steam turbines, power generator, nuclear power plant and other types of power machinery. A fatigue failure mostly begins at a local discontinuity, and when the stress at the discontinuity exceeds elastic limit, there is plastic strain. The cyclic plastic strain is responsible for crack propagation and fracture. Low cycle fatigue is usually characterized by the Coffin-Manson relation as follows:

$$\Delta\varepsilon_p/2 = \varepsilon'_f (2N)^c \quad (1)$$

Where, $\Delta\varepsilon_p/2$ is the plastic strain amplitude; ε'_f is the fatigue ductility coefficient, the failure strain for a single reversal; $2N$ is the number of strain reversals to failure (N cycles); c is an empirical constant known as the fatigue ductility exponent, commonly ranging from -0.5 to -0.7 for metals. The graphical representation of Coffin-Manson relation is shown in Fig. 2.3. Slopes can be steeper in the presence of environmental interactions. Low number of cycles lead to produce failure, i.e. $N < 10^4$.

During cyclic loading hysteresis loops get generated as a response of stress and strain. Figure 2.4 [11] shows a typical plot of cyclic hardening/softening behavior in LCF. It is clear from the figure that cyclic softening occurs when stress amplitude decreases. Whereas, cyclic hardening occurs when stress amplitude increases with increase in number of cycles. The change of the hardening/softening behavior of the material can be understood from the hysteresis loops. The stress amplitude value changes only in initial phases of fatigue life and then remains constant depicting cyclic stress-strain response of the material.

2.3.2 High cycle fatigue

High cycle fatigue (HCF) is generally called for high frequencies in excessiveness of around 1kHz. A prominent definition is kept away from purely elastic behavior related with HCF while LCF implies cyclic plasticity. During HCF, alternating load may be such that the maximum stress should not be greater than the 2/3 of the yield stress of the material. Thus in this case number of cycles to failure is important to know at relatively low stress. HCF is generally carried out in load or stress control mode while LCF is usually carried out in strain controlled condition. In contrast to HCF the LCF studies are generally thought to be occurred from thermal origin where a component gets strained. Thus in this case strain, rather than stress, is more important. This is the reason for which LCF is generally done at strain controlled mode. There is no conventional definition, but HCF generally includes high frequencies, nominally elastic cyclic behavior, low amplitudes, and endures large numbers of cycles.

2.4 Effect of mean stress on fatigue

Plenty of research was carried out by investigators to understand the fatigue behavior with completely reversed cycles (zero mean stress). But only scattered information is available for deciding an S-N graph for a circumstance where the mean stress is not equal to zero. Figure 2.5 (Haig-Soderberg curve) demonstrates the plans that are utilized to make note of mean stress in depicting the endurance limit. The Goodman relation gives a good result for brittle materials and conservative results for ductile materials.

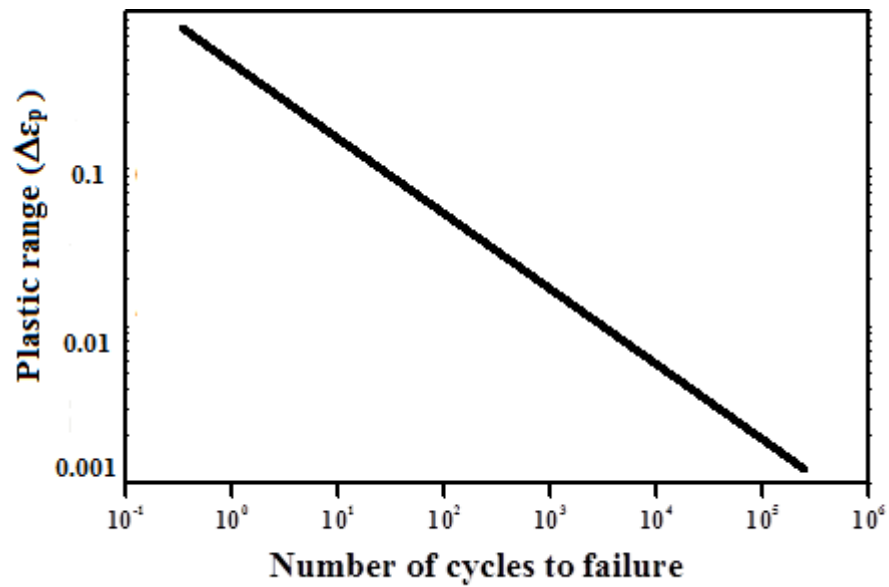


Fig. 2.3: Graphical representation of Coffin-Manson relationship.

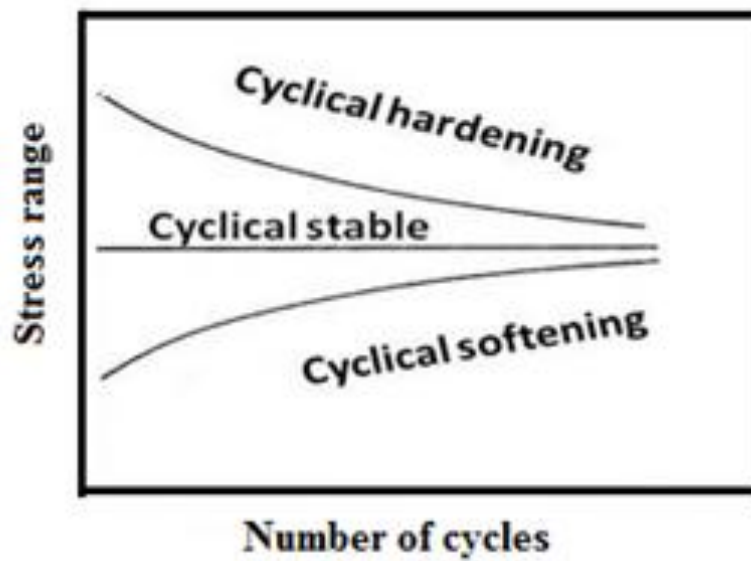


Fig. 2.4: Plot of cyclic hardening/softening behavior in low cycle fatigue. [11]

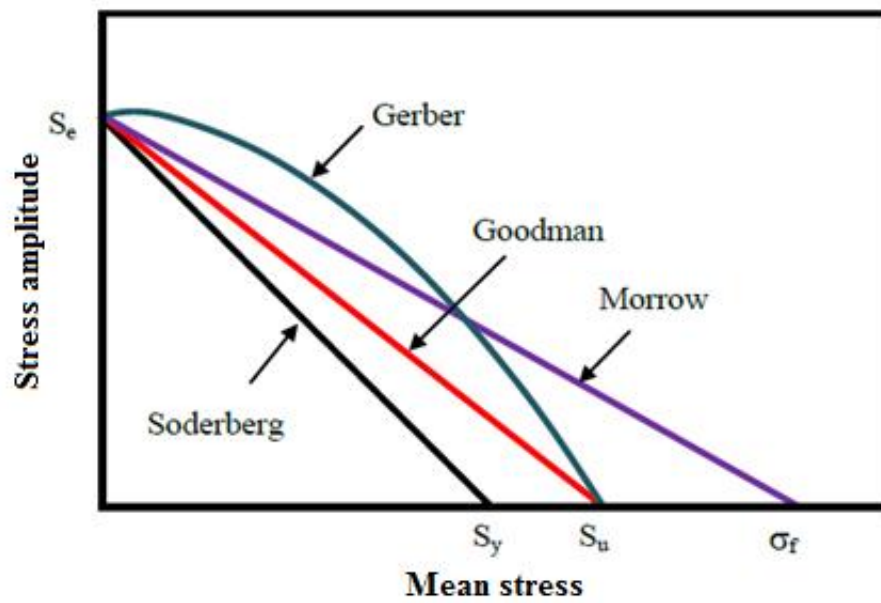


Fig. 2.5: Effect of mean stress on endurance limit (schematically drawn by seeing the nature of similar plot given in reference [1]).

The Gerber relation gives good results for a ductile material. Fatigue strength of a component tends to increase with compressive mean stress and decrease in tensile mean stress. Gerber's parabolic relationship, yield an erroneous answer to the conservative side in the compressive mean stress region.

2.5 Ratcheting

Ratcheting is an important phenomenon during the study of fatigue failure of engineering materials at their services. Ratcheting is defined as the phenomenon of strain accumulation during asymmetric cyclic loading of materials under application of non-zero mean stress at different stress amplitudes [12-13]. It is known that ratcheting deformation occurs when hysteresis loops produced for subsequent cycles translate towards higher plastic strain. The schematic diagram of the ratcheting procedure is presented in Fig. 2.6. Ringsberg [14] stated that ratcheting is instances where it exhibits additional plastic deformation during every load cycles and strain accumulates continuously. The strain accumulation of a material can be mathematically calculated as the average of maximum and minimum strain [15-18]; it can be expressed as:

$$\varepsilon_r = (\varepsilon_{\max} + \varepsilon_{\min})/2 \quad (2)$$

Where, ε_r = axial ratcheting strain

ε_{\max} = maximum strain at a particular cycle

ε_{\min} = minimum strain at that cycle.

Ratcheting plays a vital role in the design of load bearing structural parts. The earlier investigations available in the literature are of Kujawski et al. [19] and Yoshida et al. [20]. In 1981 Yoshida et al. [21] explained a uniaxial ratcheting model used to calculate ratcheting strain on the basis of biaxial stress cycles using equivalent ratcheting strain. In 1990, Yoshida [22] reported the impact of stress ratio on uniaxial and multi-axial ratcheting strain accumulation in SUS304 stainless steel at room temperature. In the same year, Ruggles and Krempl [23] showed the interaction between cycling hardening and ratcheting for AISI 304 stainless steel. Hassan and Kyriakides [24] investigated the ratcheting behavior of hardenable and softenable materials under uniaxial cyclic loading. Xia et al. studied the effect of mean stress and ratcheting on the fatigue life of steel in the year 1996 [25].

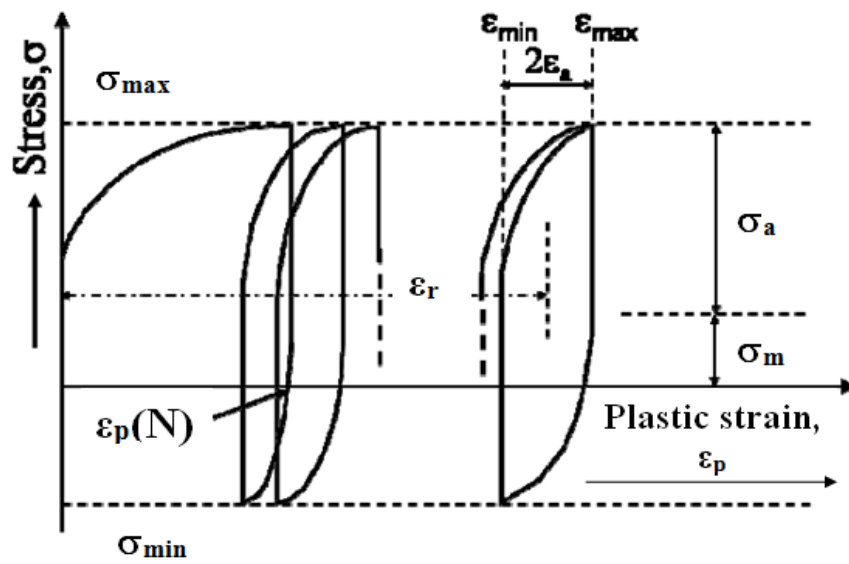


Fig. 2.6: Schematic representation of ratcheting phenomenon.

2.6 Factors affecting ratcheting

There are various factors that affect strain accumulation during ratcheting. These factors are the maximum stress, mean stress, stress ratio, temperature, pre-strain, etc. Two of the relevant factors are discussed here.

2.6.1 Pre-strain

In 2007 Kang et al. [26] studied the effect of pre-strain on ratcheting behaviour of carbon steel. They reported that the fatigue life of 0.1% carbon steel increased with increasing surface hardness and surface compressive residual stress imposed by pre-strain. Simultaneously, in the case of 0.5% carbon steel fatigue life decreased when pre-cracks were generated on the large surface compressive residual stress. In 2011, Paul et al. [27] investigated the cyclic plastic deformation behavior in SA333 Gr. 6 C–Mn steel and concluded that in cyclic hardening/softening behavior when the material is pre-strained and then subjected to LCF tests, the stress amplitude is found to decrease with cycling i.e. cyclic softening occurs. In 2013, Wang et al. [28] studied the effects of pre-strain on uniaxial ratcheting and fatigue failure of Z2CN1810 austenitic stainless steel and reported that ratcheting strain of subsequent stress cycling decreases with increasing tensile pre-strain. In 2014 De et al. [29] interpreted the effect of pre-strain on post ratcheting tensile properties of Ti-stabilized interstitial free steel. They concluded that yield strength increases in two distinctly different stages; the increase of tensile strength follows perfect linear relationship with the increase in the amount of pre-strain. The effect of monotonic and cyclic deformation on the evolution of back stress vis-à-vis Bauschinger effect due to different amounts of unidirectional plastic deformation in annealed OFHC copper has been investigated in 2014 by Mahato et al. [30]. They concluded that higher back stress develops in the case of monotonic deformation as compared to ratcheting deformation, for the same amount of unidirectional pre-strain. They also found that the effect of stress rate on the change of Bauschinger parameters is comparatively less than the effect of increasing pre-strain in both types of deformation. Investigation on the effect of tensile pre-strain on ratcheting behavior of 430 Stainless steel under fully-reversed loading condition was done by Chiou et al. [31] and they concluded that fatigue life decreases with increasing the tensile pre-strain level.

2.6.2 Corrosion-Fatigue

Effect of corrosion on fatigue of materials has been studied by numerous researchers [32-35]. Investigations on corrosion fatigue subjected to different material/environment combinations and experimental variables show that the corrosion environment significantly decreases the fatigue strength and life, and even leads to the absence of the fatigue limit [36-43]. Zhao et al. studied the mechanism of high-cycle corrosion fatigue crack initiation in X80 steel in 3.5% NaCl solution and reported that the corrosion fatigue crack initiation was due to the corrosion pits and the adhering corrosion products [44]. Similarly Rezig et al. investigated the development of early cracks in high strength stainless steel in 5% NaCl solution and concluded that cracks initiated at their largest K_t values [45]. Grilli et al. also worked on corrosion of a 2219 aluminum alloy exposed to a 3.5% NaCl solution and confirmed that the corrosion products rich in aluminum and oxygen were found to progressively accumulate around the particles and iron was dissolved from the intermetallic, followed by back deposition [46]. Investigations were also done on the corrosion fatigue crack growth in AISI 4340 steel using pre-cracked compact tension specimens in dry air, distilled water, and 3.5% NaCl aqueous solution at different R-ratios and different loading frequencies by Weng et al. [47]. They reported that the material displayed typical type B corrosion fatigue crack growth behavior. Meng et al. [48] investigated corrosion fatigue crack growth rate in 7075 aluminum alloy in sea water and concluded that corrosion solution concentration, pH value, temperature, and load frequency have great influence on corrosion fatigue crack growth rate. The fracture surface indicated that the corrosion pits extending along the direction of the crack growth are responsible for the acceleration of the crack growth rates. Scanning Kelvin Probe Force Microscopy results proved that large potential differences between iron-containing intermetallics and α -Al matrix were responsible for the initiation of attack at the intermetallics/ α -Al interfaces due to corrosion and corrosion resistance increased in the rheocast A356 aluminum alloy as proposed by Arrabel et al. [49].

2.7 Reappraisal of the current problem

ASTM A668 class D steel is a plain carbon steel which is potentially being used in various engineering sectors as discussed in chapter 1. In all such applications, a clear idea regarding the tensile, fatigue and fracture behavior of the material is of utmost importance. Fatigue may be regarded as the most important property requirement for proper designing and safety concern of structural components. A thorough review of the literature related to the current steel under investigation shows that properties like tensile, fracture etc. and impact behavior of the steel were studied by earlier investigators. The effect of pre-strain on ratcheting behaviour of other plain carbon steels were investigated [26]. However, the ratcheting behavior of ASTM A668 class D steel with the effect of pre-strain has not been studied till date. Moreover in some of the critical applications of the material corrosion becomes an important aspect. Effects of corrosion on fatigue of different materials have been studied by numerous researchers [32-35]. But as per the best knowledge of the author no report exists in literature to study the effect of pre-strain and pre-corrosion on ratcheting behavior of ASTM standard A668 class D steel. The present investigation intends to fulfill this gap.

Chapter 3

Experimental Procedure

As discussed in previous chapter that the aim of the study is to investigate ratcheting fatigue behavior of ASTM A668 class D steel in different heat treated conditions as well as following pre-corrosion. For this the material was characterized for its chemical composition, microstructure as well as tensile and hardness properties. The ratcheting tests on the material were done based on the obtained tensile strength of the material subjected to different heat treatments. Detailed descriptions of all these experiments are provided in the following sections.

3.1 Material selection

The material selected for this investigation is Class D steel of ASTM standard A668. It was available in the form of an ingot of dimension $120 \times 65 \times 55 \text{ mm}^3$. The chemical composition of the material as assessed using optical emission spectrometer (Model: ARL 3460 Metals Analyzer) is shown in Table 3.1.

Table 3.1: Chemical composition of the investigated ASTM class D steel

Element	C	Mn	P	S	Si	Fe
Wt%	0.35	0.90	0.04	0.04	0.35	Balance

3.2 Heat treatment

In this investigation, two different heat treatments like normalizing and hardening-tempering were adopted. The steel was cut into pieces of suitable size so as to minimize wastage of material and optimize heat treatment of the part. In next two sections the detailed descriptions of these treatments are given.

3.2.1 Normalizing

- Samples were heated upto a predetermined temperature of 860°C in muffle furnace. This temperature was chosen based on the corresponding AC_3 (820°C) temperature of the steel plus 40°C.
- The heat treated samples were soaked at this temperature for 2 hrs to obtain homogeneous structure.
- Air cooling of samples upto room temperature.

3.2.2 Hardening and tempering

- Heating the samples to a predetermined temperature of 860°C.
- Soaking at 860°C for 2 hrs to obtain homogeneous structure.
- Quenching of samples in water.
- Re-heating of the samples to a predetermined temperature of 600°C.
- Soaking at 600°C for 4 hrs followed by slow cooling at muffle furnace.

3.3 Microstructural characterization

For microstructural studies samples of 10 mm height were cut from the normalized and hardened tempered steels. Then the samples were ground roughly by high speed belt grinder. After belt grinding, different grades of emery paper were used to polish the samples (upto 1000 grit). Then the samples were polished by using wet rotating wheel covered with special cloth that was coated with abrasive (alundum). After this samples were cleaned with soap solution, and then the samples were dried using drier. Finally these samples were then polished using diamond paste up to 0.25 μ m surface finish. Then the specimens were etched with freshly prepared 5% nital solution. The samples were finally examined by optical

microscopy (Model: Olympus BX61, Tokyo, Japan) and images were captured at different magnifications.

3.4 Mechanical testing

3.4.1 Hardness testing

Samples of approximate dimension of $10 \times 10 \times 10 \text{ mm}^3$ were cut from the as received and heat treated steel for determination of Vickers hardness. A load of 10kgf and a dwell time of 10s were set for the measurements.

3.4.2 Tensile testing

The tensile tests were done using ASTM standard E8M (2014) [50]. For this cylindrical samples were cut which had 6mm gauge diameter and 25 mm gauge length. The tests were conducted at room temperature using a universal testing machine (Model: Instron 1195, Birmingham, UK) at 1 mm/min cross head speed and this speed corresponds to nominal strain rate of $6.66 \times 10^{-4} \text{ s}^{-1}$. The fractured samples were preserved for fractography. The load and displacement values for each tensile test were recorded and these recorded values were used to prepare load vs. displacement graphs and subsequently engineering stress-strain curves. A particular configuration of a typical tensile specimen is shown in Fig. 3.1.

3.5 Ratcheting study

The heat treated steel blocks were machined as per ASTM E606 [51] to fabricate samples (diameter 6mm and gauge length 12.5 mm) for ratcheting tests. Stress controlled LCF tests were carried out using $\pm 100 \text{ kN}$ universal testing machine (Model: BISS, Bangalore, India). All these tests were done at room temperature at a constant stress rate of 50 MPa/s and for 100 cycles. The tests can be classified into three categories (i) effect of pre-strain on ratcheting behavior of normalized steel (ii) effect of pre-strain on ratcheting behavior of hardened-tempered steel (iii) ratcheting tests on pre-corroded steel samples. A schematic drawing of a specimen for ratcheting test is illustrated in Fig.3.2. Before doing the ratcheting tests, the specimens were subjected to different pre-strain levels of 2%, 4% and 8% (strained at a nominal strain rate of 0.001 s^{-1})

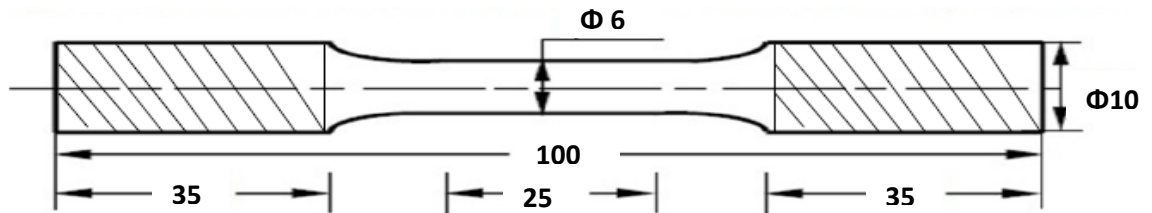


Fig. 3.1: Sample design for tensile test.

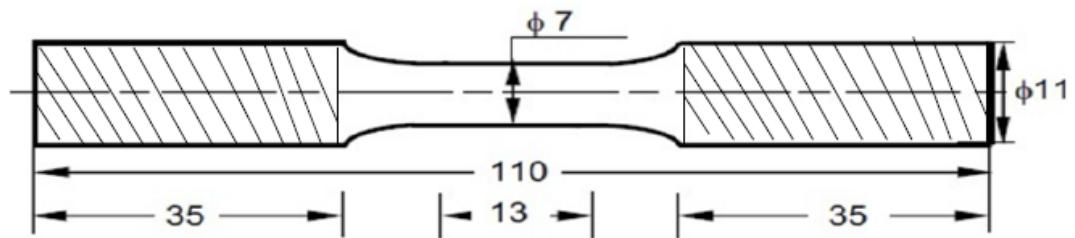


Fig. 3.2: Sample design for fatigue study.

The maximum stress values for cyclic loading were chosen about 50% of the ultimate tensile stress values. Generally tests are done above the yield strength but in this case, in order to know the strain accumulation below the yield strength level the stress parameters were chosen in this manner. The minimum stress values for normalized steel was -150 MPa and -200 MPa for hardened-tempered steels. The nature of strain accumulation was also examined for specimens without pre-strain, which is designated as 0% pre-strain level. It is understood that the microstructure of a material can alter its deformation behavior and thus, the nature of strain accumulation due to ratcheting must be dependent on the microstructural constituents. One of the major application of the steel in hardened-tempered condition is in hydro turbines, where ratcheting is a major problem. Therefore, a set of samples were hardened-tempered and tested for the effect of pre-strain on strain accumulation due to ratcheting. The maximum stress for normalized samples was 265 MPa and that for hardened-tempered specimens was 328 MPa.

3.6 Corrosion-fatigue test

A set of normalized samples were subjected to corrosion for 7, 14 and 21 days in saline water. The saline water was prepared by dissolving 3.65% NaCl in one liter of distilled water. A schematic drawing of the entire set up is shown in Fig.3.3. The gauge portion of the specimen was dipped in NaCl solution to impose different amount of corrosion to the specimens. Proper precautions were taken to avoid any degradation of the threaded part by coating it with protective coating followed by wrapping it using plastic tapes. After the removal of the specimens from the solution, these were dried and wrapped in aluminum foil and kept in desiccator to avoid further corrosion. Ratcheting tests were done on these samples to understand the nature of strain accumulation with different levels of pre-strains.

3.7 Post ratcheting tensile test

Tensile tests on the ratcheted samples (all the samples other than pre-corroded have been carried out) to study the extent of cyclic plastic damage. The post ratcheting tensile tests were carried out using the procedure as mentioned in section 3.4.2. The obtained load and displacements data were used to calculate the corresponding stress strain values. Figure 3.4. shows a broken post ratcheting tensile specimen.

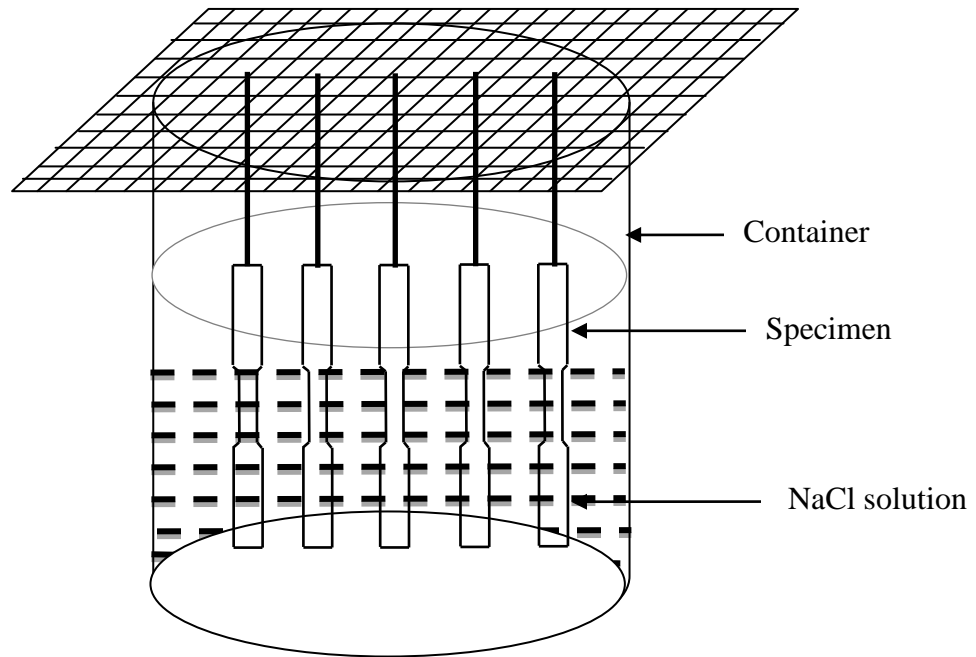


Fig. 3.3: Schematic representation of the set up used to introduce in the samples.



Fig. 3.4: Photograph of a broken post ratcheting tensile sample

Chapter 4

Results and Discussion

In this chapter the results obtained during characterization and study of ratcheting behavior of A668 class D steel are presented and discussed elaborately. The following chapter can be broadly classified into two parts; first being the results and pertinent discussion on the basic characterization of the material which includes the microstructural analyses, hardness and tensile tests. The other part of the thesis consists of the results and discussion on the ratcheting behavior of the material at two different heat treatment conditions in samples which were pre-strained at different levels before the cyclic loading operation plus the results and discussion of ratcheting tests on pre-corroded samples.

4.1 Microstructural analysis

The microstructural analysis of the investigated steel under normalized and hardened-tempered conditions are shown in Fig. 4.1. Figure 4.1 (a) depicts the optical microstructure under normalized condition which shows the presence of ferrite and pearlite, as expected. The microstructure of the steel under hardened-tempered condition consists of tempered martensite as shown in Fig. 4.1 (b). It is known that tempered steel contains tempered martensite as well as different carbides like ϵ , η carbide and cementite [52]. However some negligibly small amount of retained austenite may also be present in the structure. It is theoretically established that austenite to martensite transformation is never complete and small amount of retained austenite remains in the structure even at low temperatures. As the amount of austenite decreases towards the ends of the particular transformation operation, the chances of total transformation of austenite becomes difficult [53]. However, it is not easy to locate the regions belong to retained austenite using optical microscopy. Thus as a whole, it can be said that the hardened-tempered microstructure contains tempered martensite.

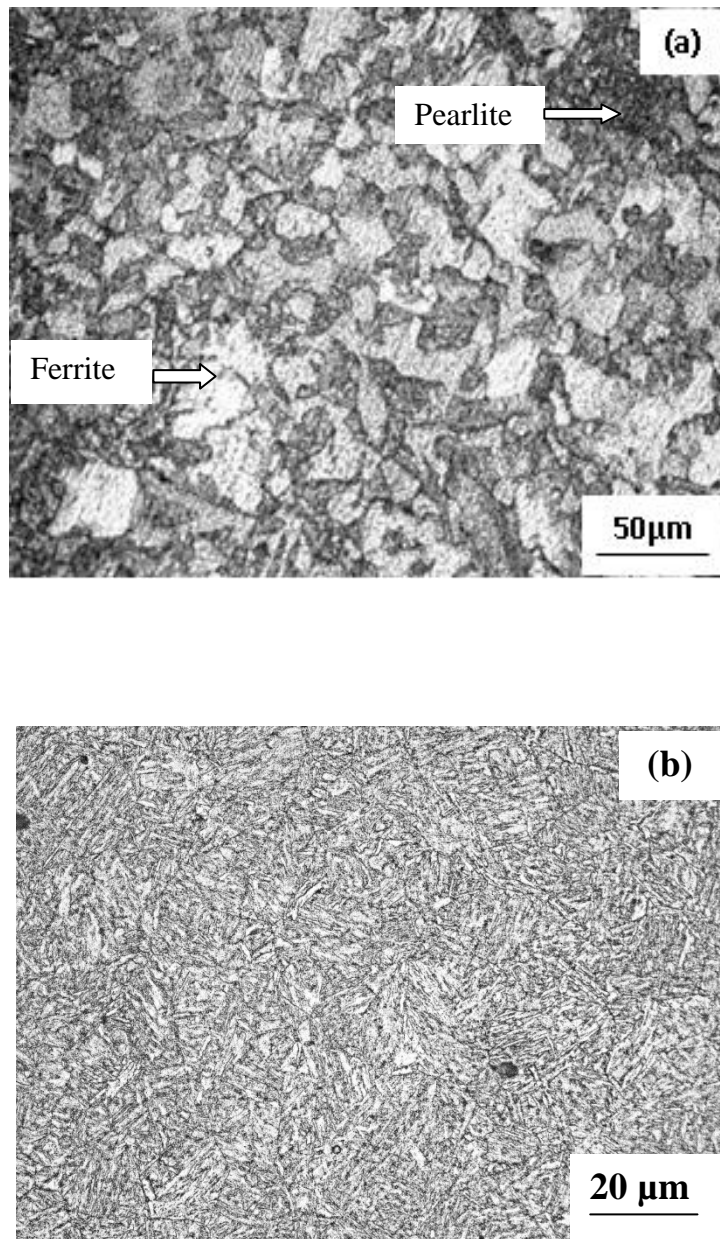


Fig. 4.1: Optical microstructures of the steel in (a) normalized and (b) hardened-tempered condition.

4.2 Hardness

The results of the hardness tests of normalized and hardened-tempered samples are shown in Table 4.1. The hardness values of normalized and hardened-tempered samples were compared and it was found that the average hardness of the hardened-tempered specimen is 155 VHN which is higher as compared to the normalized specimen with average hardness of 128 VHN.

Table 4.1: Vickers hardness values of the normalized and hardened-tempered samples of the investigated A668 Steel.

Serial No.	Normalized		Hardened-tempered	
	VHN (10)	Average (VHN)	VHN (10)	Average (VHN)
1	123.9	128±3.83	152.7	155±3.68
2	129.6		159.4	
3	131.2		153.4	

4.3 Tensile behavior

The tensile properties of the investigated steel were studied by using the heat treated (normalized and hardened-tempered) cylindrical samples. The procedure of the tensile test is given in section 3.5. Figure 4.2 (a) and (b) depicts the typical engineering stress-strain curves of the investigated steel for normalized and hardened-tempered conditions. It can be seen continuous yielding from elastic to plastic region has occurred. Thus, the yield strength was estimated by 0.2% strain off-set procedure as given in ASTM E8M [54]. The tensile properties of the normalized and hardened-tempered samples are given in Table 4.2. All the values which are tabulated are almost near to standard values of this particular steel as mentioned in ASM hand book .Hence it can be stated that the heat treatment and specimen design of investigated steel were proper. By estimating the stress values from the above stress strain plots for normalized and hardened-tempered specimens and comparing the results, the yield strength and ultimate tensile strength of the normalized specimen were

found to be 359 MPa and 545 MPa which is less as compared to the hardened-tempered specimen which were 466 MPa and 650 MPa respectively. This fact shows that the hardened-tempered specimen has more strength compared to normalized specimen because hardened-tempered steel is composed of tempered martensite and carbides that is having higher strength as expected. The uniform elongation of normalized specimen was found as 0.5% and for hardened-tempered specimen was 0.4%. The total elongations of normalized specimen and hardened-tempered specimens were 34% and 30% respectively. From the above results it can be concluded that the hardened-tempered specimen is less ductile and as compared to normalized specimen. The strain hardening exponent (n) values were calculated by using Hollomon equation $\sigma = K\varepsilon^n$, where ' σ ' and ' ε ' are true stress and true strain respectively while ' K ' is strength coefficient. The ' n ' values of the steel were estimated from the slope of the log-log plot of true stress and true strain. The log (σ) vs. log (ε) plots for hardened-tempered samples resulted into straight lines are given in Fig. 4.3 (a) and (b). The strain hardening exponent values of the samples in both heat treated conditions are given in the Table 4.2. A comparison of ' n ' values indicates that the hardened-tempered steel is having lower ' n ' value than the normalized steel. As the normalized steel can be treated as softer than the hardened-tempered steel, the rate of strain hardening is more in normalized steel during tensile deformation, and thereby the magnitude of ' n ' has increased. Initially, hardened-tempered steel did not further harden much, resulting lower ' n ' value.

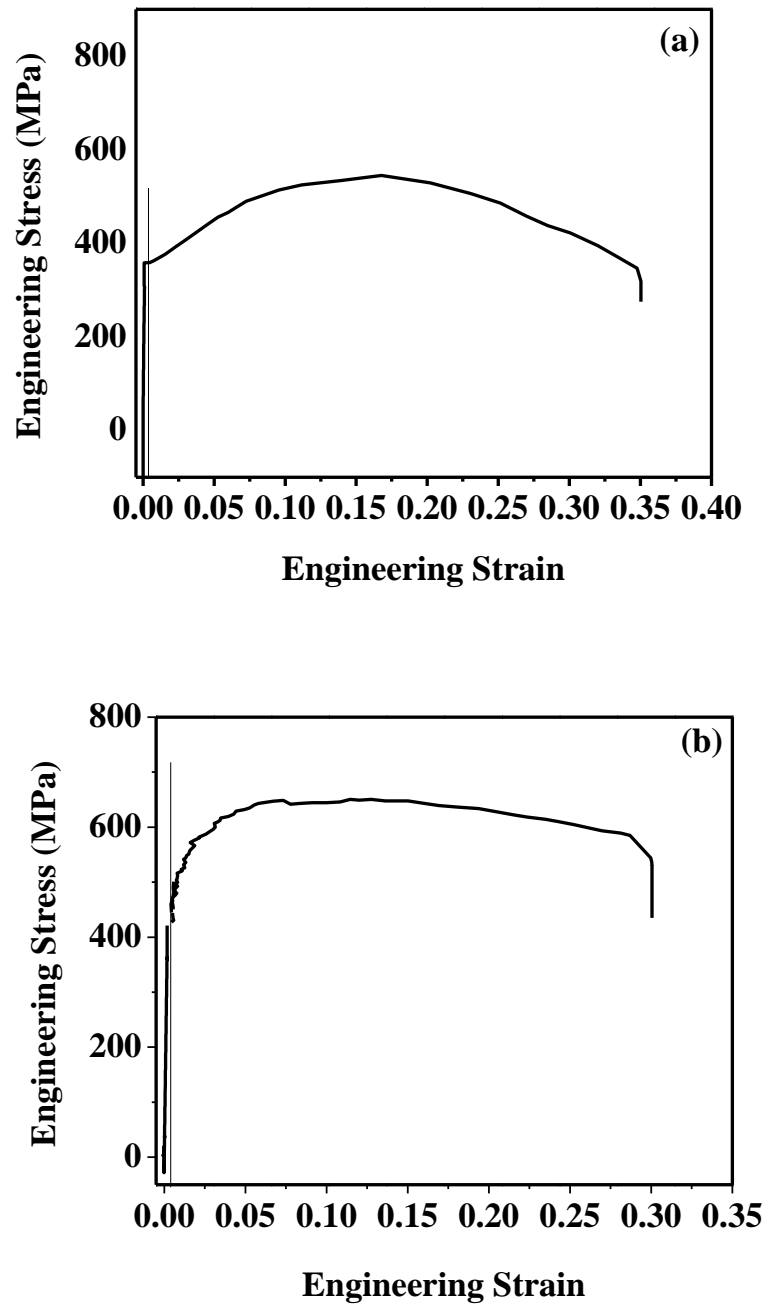


Fig. 4.2: Engineering stress-strain curves of (a) normalized and (b) hardened-tempered samples of the investigated steel.

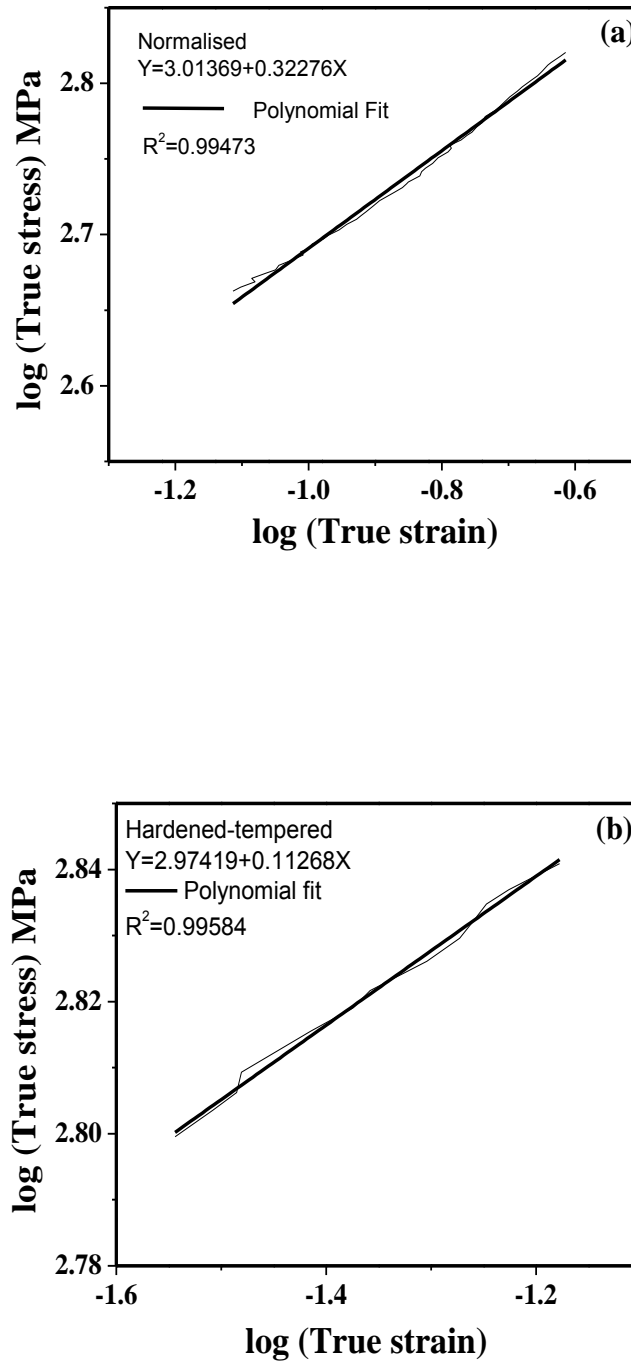


Fig. 4.3: (a) Typical $\log(\sigma) - \log(\epsilon)$ plots for normalized and (b) hardened-tempered samples of ASTM Class D A668 Steel.

Table 4.2: Tensile properties of the investigated steel

	Normalized	Hardened-tempered
Yield strength (MPa)	359	466
Ultimate tensile strength (MPa)	545	650
Uniform elongation	0.004	0.005
Total elongation	0.34	0.30
Strain hardening exponent (n)	0.32	0.11

4.4 Ratcheting behavior

4.4.1 Effect of pre-strain on ratcheting behavior of normalized steel

It is known from several earlier reports that accumulation of ratcheting strain attains a saturation level (the details of which is given in section 4.4.3) after few cycles of deformation. The saturation level for ferrous materials is around 100 cycles. Significant amount of structural variations occur upto this saturation level and hence it was decided for the current study that all ratcheting tests would be done upto 100 cycles. The results of cyclic tests conducted up to 100 cycles under various pre-strain levels (0%,2%,4%,8%) in normalized conditions are presented and discussed in this section. The nature of accumulation of ratcheting strain with number of cycles under various pre-strain levels is represented in Fig. 4.4 (a) while Fig. 4.4 (b) illustrates the types of stress-strain hysteresis loops for a pre-strain level of 0%. It can be noted from Fig. 4.4 (a) that accumulation of ratcheting strain decreases with increasing the level of pre-strain. The accumulation of ratcheting strain increases with increase in number of cycles while for most metals, strain saturation occurs after certain duration. The investigated steel attains a saturation level after about 20 cycles; this is discussed in more detail in a later section. Strain accumulation is maximum when there is no pre-strain (0%, as indicated in the figure). It is noted that the strain accumulation can vary from 0.21 % to 0.44 % with decreasing pre-strain. This kind of variation in strain accumulation can be attributed to the dislocation distribution happens during pre-straining. The dislocations pile up during the pre-straining and the extent of dislocations in a pile up increases with the increase in the level of pre-strain. Wang et al. [28] reported that if the level of pre-strain is increased, these dislocation pile ups generate some back stress which hinders to accumulate strain during subsequent ratcheting deformation. The extent of back stress increases with pre-strain and accordingly accumulation of

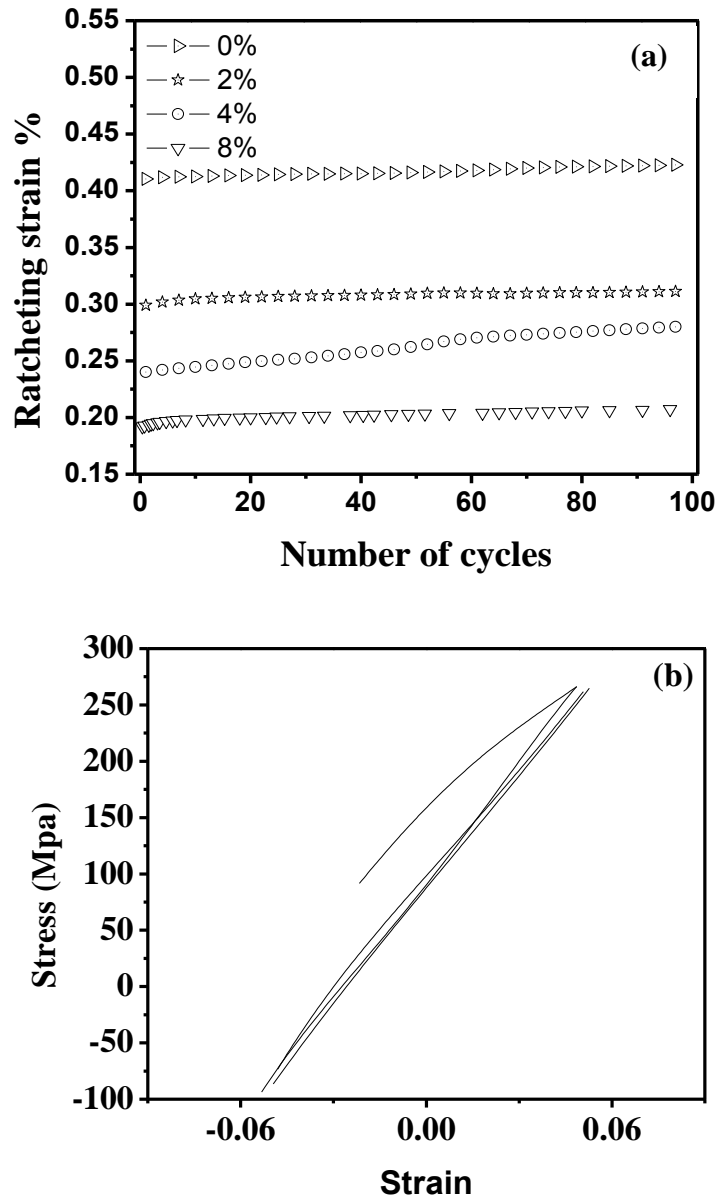


Fig. 4.4: (a) Effect of pre-strain on accumulation of ratcheting strain and (b) hysteresis loops produced during ratcheting with no pre-strain in normalized steel.

ratcheting strain gets reduced during a test done with positive mean stress. The decrease of ratcheting strain with increase in pre-strain is in accordance with the results reported by De et al. [29] for their studies on IF steel. They reported that during asymmetric cyclic loading, evolution of ratcheting strain occurs in the compressive direction as long as back stress overpowers the imposed tensile mean stress. On continued cycling the effect of back stress is exhausted, because of unlocking of dislocations from different barriers along with associated change in the dislocation substructure. Hence the imposed mean stress gradually becomes effective with softening of the pre-deformed structure through generation of (mobile) dislocations. These dislocations get piled up against different kinds of barriers resulting in the development of back stress. When the conflict between the imposed tensile mean stress and back stress is neutralized, the cumulative accumulation rate of ratcheting strain becomes zero, and at this condition the cumulative compressive ratcheting strain becomes maximum. The variation in strain range in stress controlled fatigue mostly depends on change in hardening or softening behaviour of the material. As it is known that, if the hysteresis loop area increases, a material shows cyclic softening behavior while the opposite dictates cyclic hardening [55-57]. This hardening/softening feature of materials depends greatly on the different pre-treatments experienced. In Fig. 4.4 (b), typical set of hysteresis loops are illustrated those produced from the conducted ratcheting tests without any pre-strain. One can note that the loops shift from its initial position towards right. This fact indicates that a considerable amount of plastic strain gets accumulated during each cycle which is the signature of strain accumulation due to stress-controlled cyclic loading. To understand the extent of plastic damage as well as cyclic hardening/softening during cyclic loading, the hysteresis loop areas were calculated. It was noticed that loop area decreases with increase in number of cycles. This indicates that the selected material shows cyclic hardening behavior. The extent of this hardening is discussed in section 4.5 in terms of variation in post-ratcheting behavior.

4.4.2 Effect of pre-strain on ratcheting behavior of hardened-tempered steel

It is understood that the properties of a material vary with its microstructure and thus the nature of strain accumulation due to ratcheting must be dependent on the microstructural constituents. One of the major applications of the steel is in hardened-tempered condition to fabricate hydro-turbines. In such application ratcheting is a major problem, but as per best knowledge of the author, no literature exists in this field. Therefore, a set of samples were hardened-tempered and tested for the effect of pre-strain on strain accumulation due to ratcheting up to 100 cycles. Typical nature of strain accumulation and hysteresis loops (0%

pre-strain) are shown in Fig. 4.5 (a) and (b) respectively. In Fig 4.5 (a) it is clearly seen that the initial certain accumulation of strain is released in successive cycles for the 0% prestrain level specimen. The strain accumulation further increases after this cycle. However the deduction or increase in strain is really very less and can be considered as experimental scatter. Analogous to the normalized samples, here also, the strain accumulation reduces with increasing the level of pre-strain. In figure 4.4 (b) and 4.5 (b) each hysteresis loop represents a maximum (ϵ_{\max}) and a minimum (ϵ_{\min}) strain value. The ratcheting strain was calculated by averaging of the respective ϵ_{\max} and ϵ_{\min} values of a particular cycle. The extent of strain accumulation however, in this case varies from 0.042% to 0.015%, with increasing the level of pre-strain. Although considerable amount of strain accumulation takes place both in normalized and hardened-tempered conditions, severity of ratcheting on normalized samples is more; while pre-strain can cause seizing of strain accumulation. The lower accumulation of strain during ratcheting in the hardened tempered samples is due to type of phases present in it. Hardened-tempered steel contains tempered martensite and carbides. These tempered martensite and carbides restrict the strain accumulation during cyclic loading. This causes less strain accumulation. Further, the ratcheting studies of hardened-tempered steel were done below the yield strength values which induced less strain.

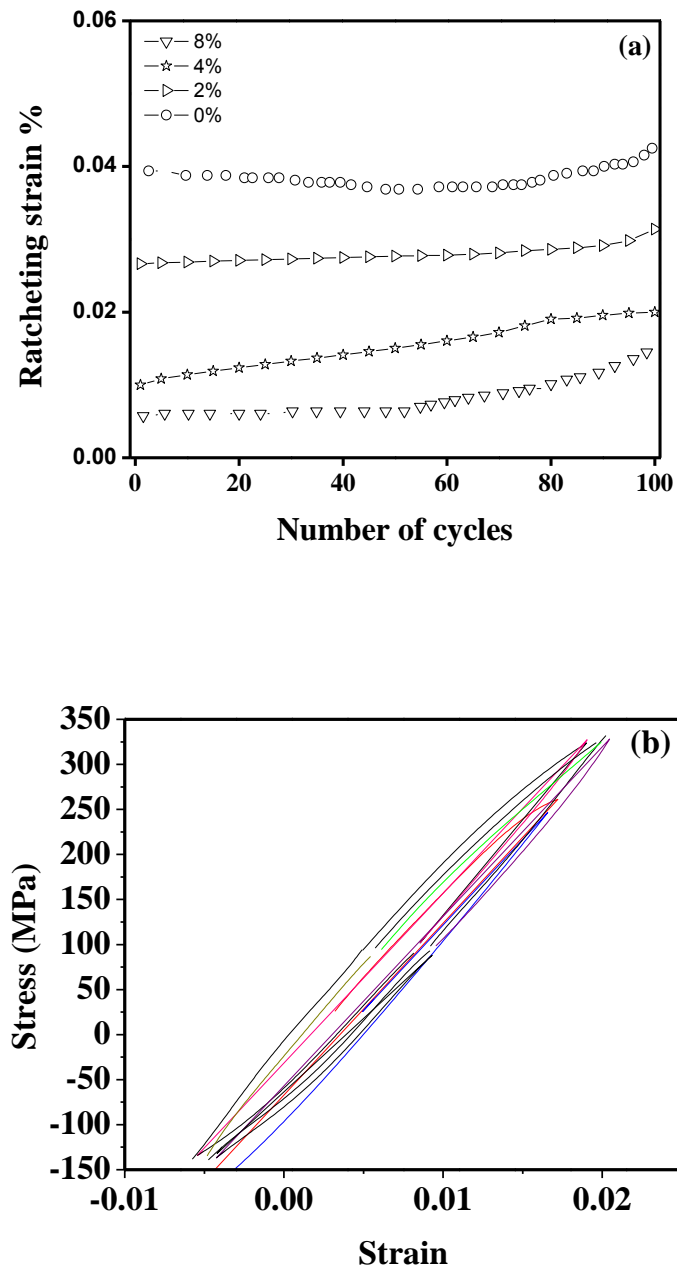


Fig. 4.5: (a) Effect of pre-strain on accumulation of ratcheting strain and (b) hysteresis loops produced during ratcheting in hardened-tempered steel.

4.4.3 Saturation in strain accumulation

It has been mentioned in several reports that rate of ratcheting strain ($d\epsilon/dN$) is observed to decrease with increasing number of cycles [58]. Initially, the rate comes down sharply, followed by an attainment of steady state in strain accumulation. This is typically similar to the nature of strain accumulation during creep deformation of a material. Occasionally, there exist three stages in the strain accumulation vs. number of cycles curves, which are designated as primary, secondary and tertiary stages. Due to the similarity of strain accumulation during ratcheting, traditionally, ratcheting was termed as cyclic creep. Dutta et al. [59] reported that rapid accumulation of ratcheting strain in the initial few cycles followed by attainment of a steady state value in ratcheting rate are the characteristic features of the asymmetric cyclic deformation behavior of a material. Figure 4.6 (a) and (b) depict the variations in rate of ratcheting strain with number of cycles in normalized and hardened-tempered conditions respectively. It can be seen from Fig. 4.6 that the rate of strain accumulation decreases continuously about 10 cycles in both normalized and hardened-tempered conditions, but this decrease is much pronounced in initial cycles. A steady state is achieved after 10 cycles, where the strain accumulation is insignificant. It was found that there is no much variation in ratcheting strain rate at different levels of pre-strain.

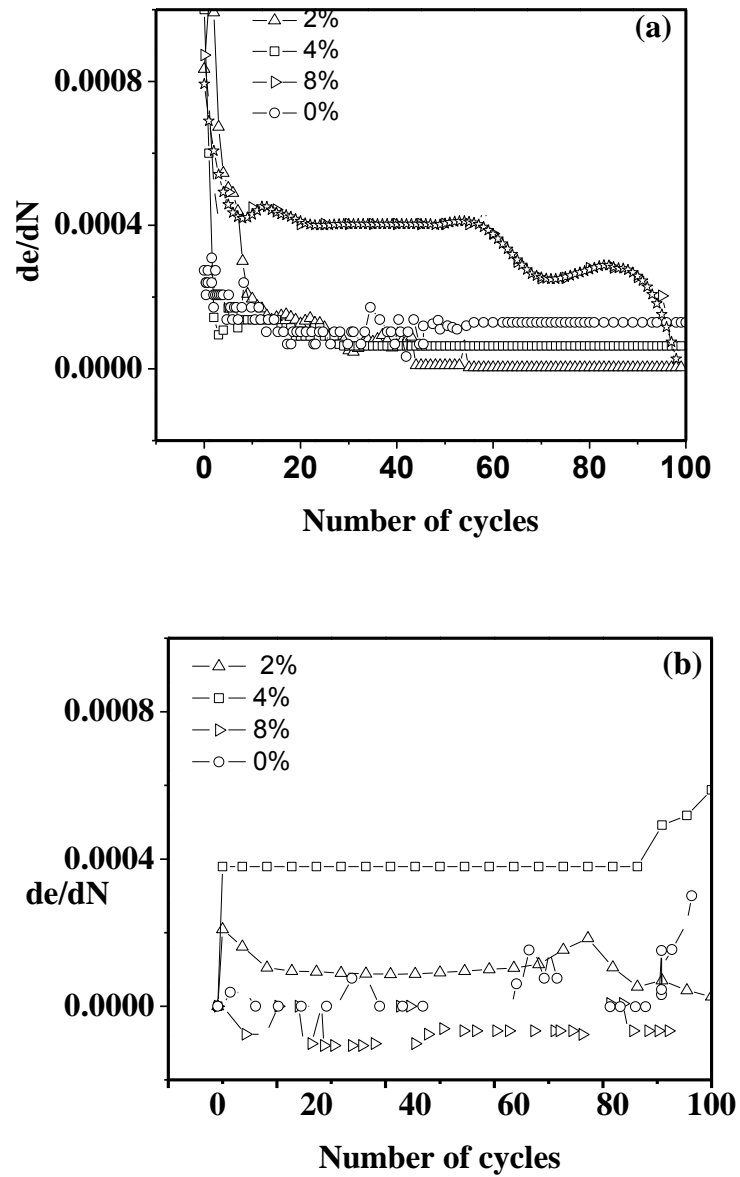


Fig. 4.6: Variations in the rate of accumulation of ratcheting strain with increasing number of cycles for (a) normalized and (b) hardened-tempered A668 class D steel at different levels of pre-strain.

4.4.4 Ratcheting tests on pre-corroded steel samples

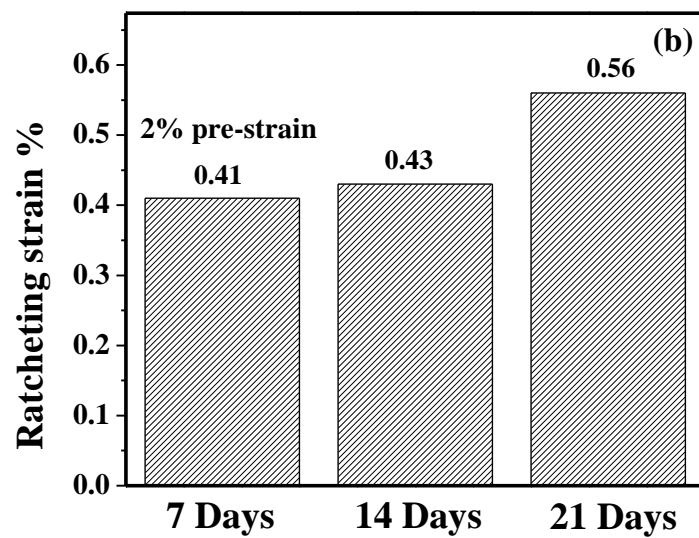
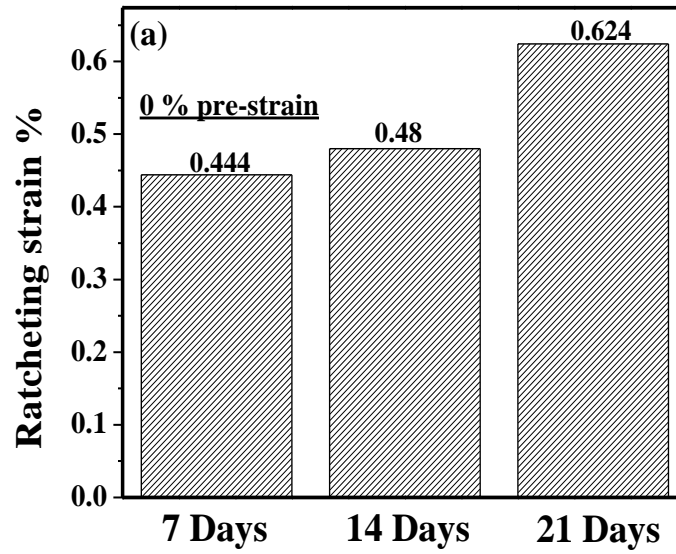
It is well known that the corrosion environment significantly decreases the fatigue strength and life of a component. It may become so severe that there may not be any true fatigue limit when a test is done under stress controlled high cycle fatigue [60]. If a crack exists in the structure, the bulk corrosion fatigue crack initiates from the pre-existing crack at low stress amplitudes. However, pits formed by the corrosive environment also contribute to initiate the crack [61-68]. Frequently, corrosion fatigue studies are done by introducing corrosive environment before the test or during the fatigue test itself. To observe the effect of pre-corrosion on accumulation of ratcheting strain, a few normalized samples were pre-corroded for different time duration and followed by ratcheting tests at different pre-strain levels. The samples were pre-corroded for 7, 14 and 21 days and it was found that corrosion pits were formed on the surface of the samples. The number density of pits increases with increasing exposure time to the environment. Typical photographs of corroded samples are illustrated in Fig. 4.7. The pits generally act as stress raisers, so it is expected that during fatigue, the crack initiation starts from these pits. Zhao et al. [44] reported that mostly corrosion fatigue initiates from the bottom of corrosion pits in X80 steel. Ryuichiro Ebara [69] also mentioned that the corrosion pits are frequently observed at crack initiation area and several micro-cracks in association with corrosion pits are observed at the surface near corrosion fatigue crack initiation area. It may thus be obvious that presence of surface pits should alter the strain accumulation behavior of a material, as that compared to a smooth specimen. Wang et al. [70] mentioned that if corrosive environment is superimposed with ratcheting deformation, the fatigue life reduces.

Ratcheting experiments under different pre-strain levels were done on the samples shown in Fig. 4.7. It was observed that strain accumulation increases at same level of pre-strain from 7 to 21 days. Figure 4.8 (a) to (d) show the comparative assessment of ratcheting strain in different levels of pre-strain. One can note that strain accumulation may reach up to 0.62% for the sample exposed for 21 days in corrosive media. It is already mentioned that the number densities of corrosion pits increases with increasing duration of exposure to the saline water. This fact leads to weakening of the samples and thus, accumulation of ratcheting strain increases. Effect of pre-strain, however, is similar to those done without the exposure of corrosive media i.e. strain accumulation reduces with increasing level of pre-strain (Fig. 4.9). However it is very interesting to note from Fig. 4.9 that, the tertiary stage appears to be present in the 21 days samples. Earlier investigations indicate that strain

accumulation during ratcheting happens in three stages (primary, secondary, tertiary) are analogous to conventional creep deformation. As the current investigation is intended to do upto 100 cycles, most of the ratcheted samples show only cyclic saturation. But unlike others, the 21 days corroded samples failed within 100 cycles, indicating three stages of ratcheting deformation. Overall, it can be stated that corrosion increases the rate of strain accumulation due to ratcheting. Better understanding of effect of corrosive media is attainable if the corrosion tests are done during the fatigue loading, however this was beyond the scope of current research.



Fig. 4.7: Corroded samples of (a)7 days (b) 14 days (c) 21 days.



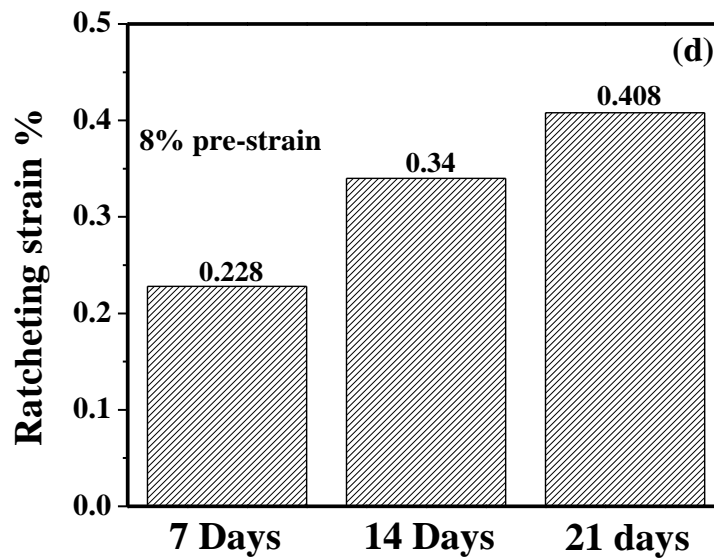
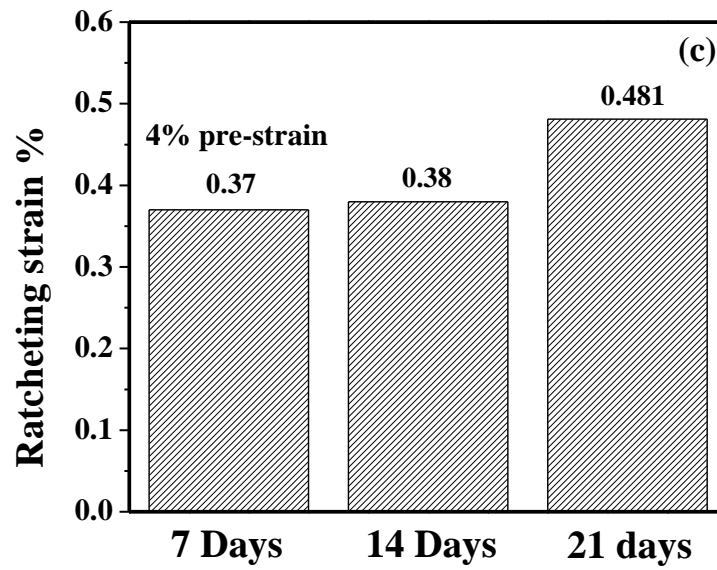
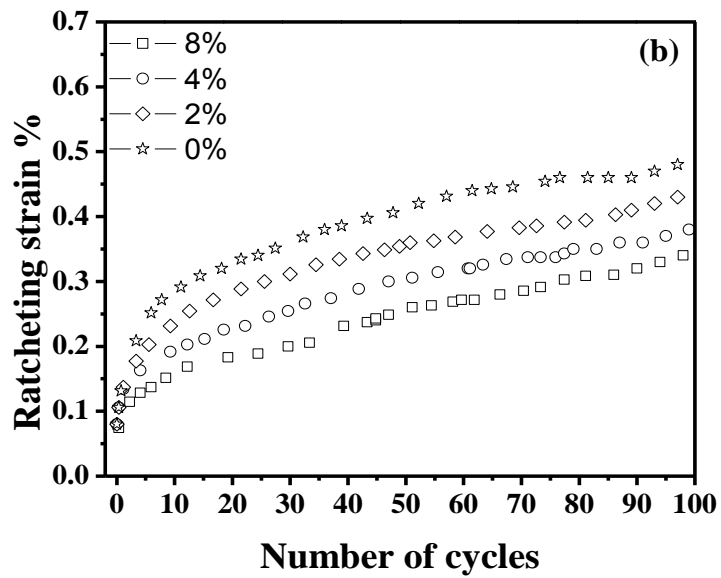
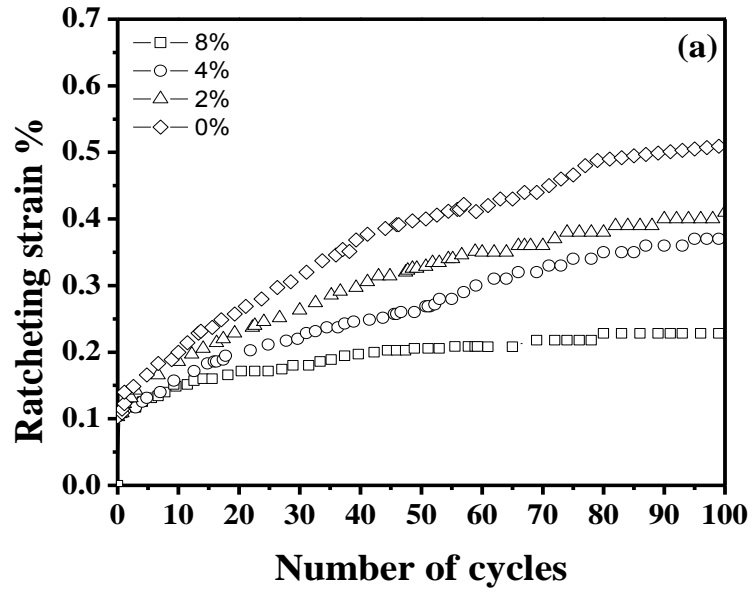


Fig. 4.8: Histogram representing ratcheting strain accumulation on corroded samples from 7 to 21 days at (a) 0% (b) 2% (c) 4% and (d) 8% pre-strain.



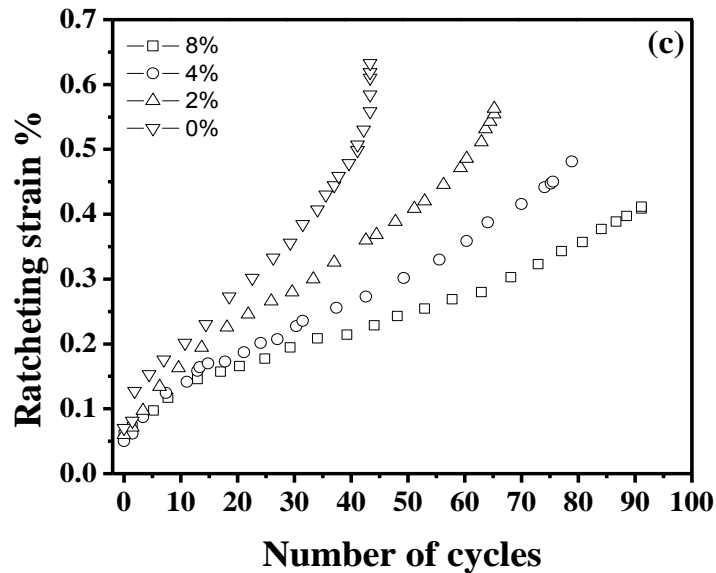


Fig. 4.9: Effect of ratcheting behavior on corroded samples for (a) 7 days (b) 14 days (c) 21 days with pre-strain.

4.5 Post ratcheting tensile behavior

It is known that ratcheting is a process of imposing plastic damage in a material; based on the nature, it gets hardened or softened during this type of ratcheting deformation. It is already discussed in previous sections that the investigated material is cyclically hardenable in nature. To further verify the features of cyclic hardening and to understand the extent of plastic damage during the course of cyclic loading, tensile tests were done on a series of specimens after imposing 100 cycles of ratcheting deformation in these. Similar works on ratcheting followed by tensile testing were reported by De et al. [29], who did post-ratcheting tensile tests on Ti-stabilized interstitial free steel, after imposing a certain percentage of ratcheting strain to the material. They reported that both yield and tensile strength increases with the amount of pre-strain in Ti-stabilised interstitial free steel. The post ratcheting tensile plots for both heat treatment conditions of the investigated steel are given in fig. 4.10 (a) and (b). The detailed results of the conducted tests are given in table 4.3. The results indicate that Y.S and U.T.S values of ratcheted specimens are higher as those compared with the unratcheted ones. But, in contrast to the results of De et al., the strength values of the

ratcheted specimens reduced with increase in the level of pre-strain. It is already discussed in previous sections that ratcheting strain decreases with the increase in pre-strain level. This fact, in turn affects the cyclic hardening process. More is the ratcheting strain in a material, more is the plastic damage and more is the cyclic hardening. The 8% pre-strain sample accumulated lowest amount of ratcheting strain and so least cyclic hardened.

The %uniform and %total elongation values of the ratcheted specimens reduced with increasing strength of material, as expected. However, with decrease in elongation values are not uniform for all the pre-strain levels. Overall, it can be stated that ratcheting deformation increases the strength of the material with marginal variations in the tensile elongation of the material.

Table 4.3: Post ratcheting tensile values for normalized and hardened-tempered samples at different levels of pre-strain.

Heat treatment	Pre-strain level	Yield strength (MPa)	Ultimate tensile strength (MPa)	Uniform elongation	Total elongation
Normalized	Unratcheted	355	530	0.29	0.77
	0%	270	710	0.10	0.67
	2%	236	682	0.33	0.63
	4%	337	665	0.15	0.55
	8%	254	589	0.31	0.74
Hardened-tempered	Unratcheted	592	655	0.10	0.71
	0%	618	882	0.16	0.39
	2%	517	857	0.34	0.46
	4%	536	710	0.10	0.60
	8%	566	688	0.11	0.63

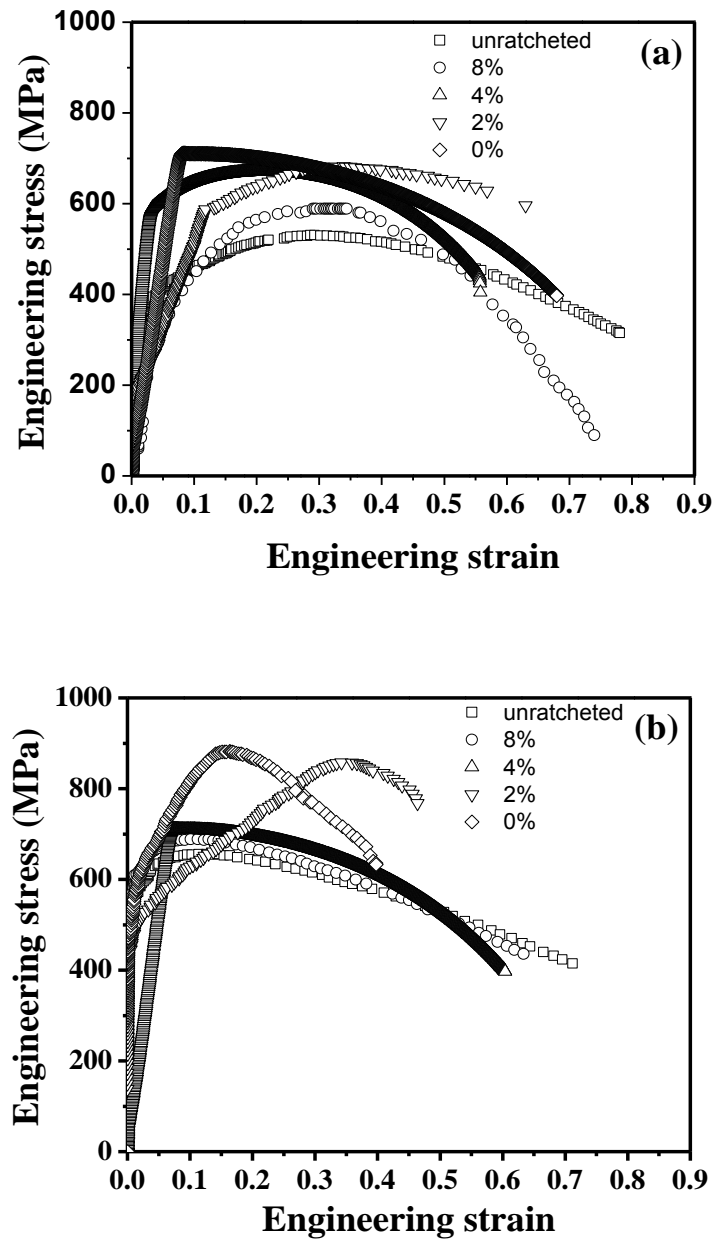


Fig. 4.10: Post ratcheting tensile stress-strain plots of (a) normalized and (b) hardened-tempered samples of investigated steel.

4.6 Fractographic observation

By using scanning electron microscope (secondary electron signal) the fracture surfaces of the broken tensile samples were tested. It is known that fracture surface carries significant evidences of the type of fracture/failure of a material. The normalized steel reveals typical cup and cone type fracture with considerable amount of necking beyond UTS. Typical fractographs of tensile fracture surfaces of the investigated steel in normalized heat treatment condition are shown in Fig. 4.11. One can note that the fracture surface is composed with ductile dimples. The mechanism of ductile fracture is well established and is known to be constituted of three successive events of void nucleation, growth and their coalescence [71, 72]. The void nucleation can take place from de-cohesion of second phase particles with its surrounding matrix, at the grain boundary triple point or if the steel is reasonably clean, then from dislocation-dislocation interaction [73]. In the present investigation, the mechanism for void nucleation in the investigated steel in normalized condition is considered to be due to de-cohesion of the particle matrix interface. The inclusions present in the investigated steel are mostly metallic carbides or sulphides, as confirmed by energy dispersive spectroscopic (EDS) analysis. Fractographs obtained from the fracture surfaces of 2% and 8% are given in Fig. 4.11 (a) and Fig. 4.11 (c) respectively. Typical EDS spectrum obtained from 2% and 8% pre-strain samples are illustrated in Fig. 4.11 (b) and in Fig. 4.11 (d) respectively. Further, it was noticed that with increasing the level of pre-strain, the dimple sizes vary. Average dimple sizes were estimated from a series of fractured samples on the normalized steel examined with different pre-strains. The average dimple size of the 2% pre-strain sample was 1.54 μm while it was 5.08 μm for the 8% sample. This fact is in direct correlation with the %total elongation obtained for the samples. The fact that %total elongation increased with increasing pre-strain, was manifested with increasing dimple size. If % total elongation increases, the required time for the failure of the specimen increases and during this time the dimple size also increases by coalescence of voids.

Scanning electron micrographs of the fracture surfaces of the broken post-ratcheting tensile specimens, which were hardened and tempered, were examined to understand the nature of fracture. Typical SEM images are shown in Fig. 4.12. The fracture surfaces of specimens primarily contain quasi-cleavage features with a few micro voids and intergranular facets as shown in Fig. 4.12. All other specimens showed similar features but with minor variations in the number of voids or intergranular facets.

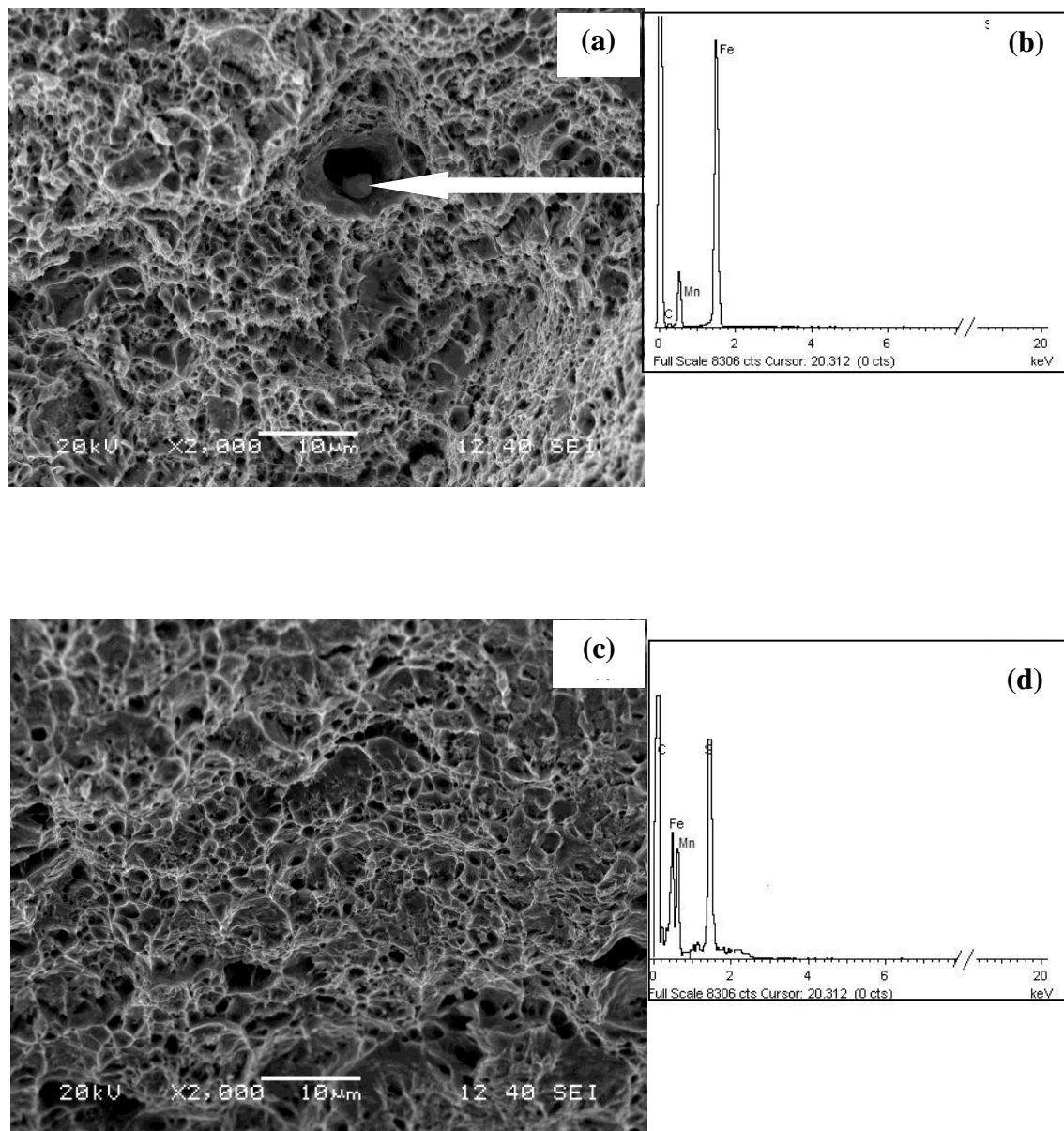


Fig. 4.11: Fracture surfaces of the broken post-ratcheting tensile specimens obtained from the normalized samples at pre-strain level of (a) 2% and (c) 8%. EDS spectrum of the corresponding fracture surfaces are given for (b) 2% and (d) 8% pre-strained samples.

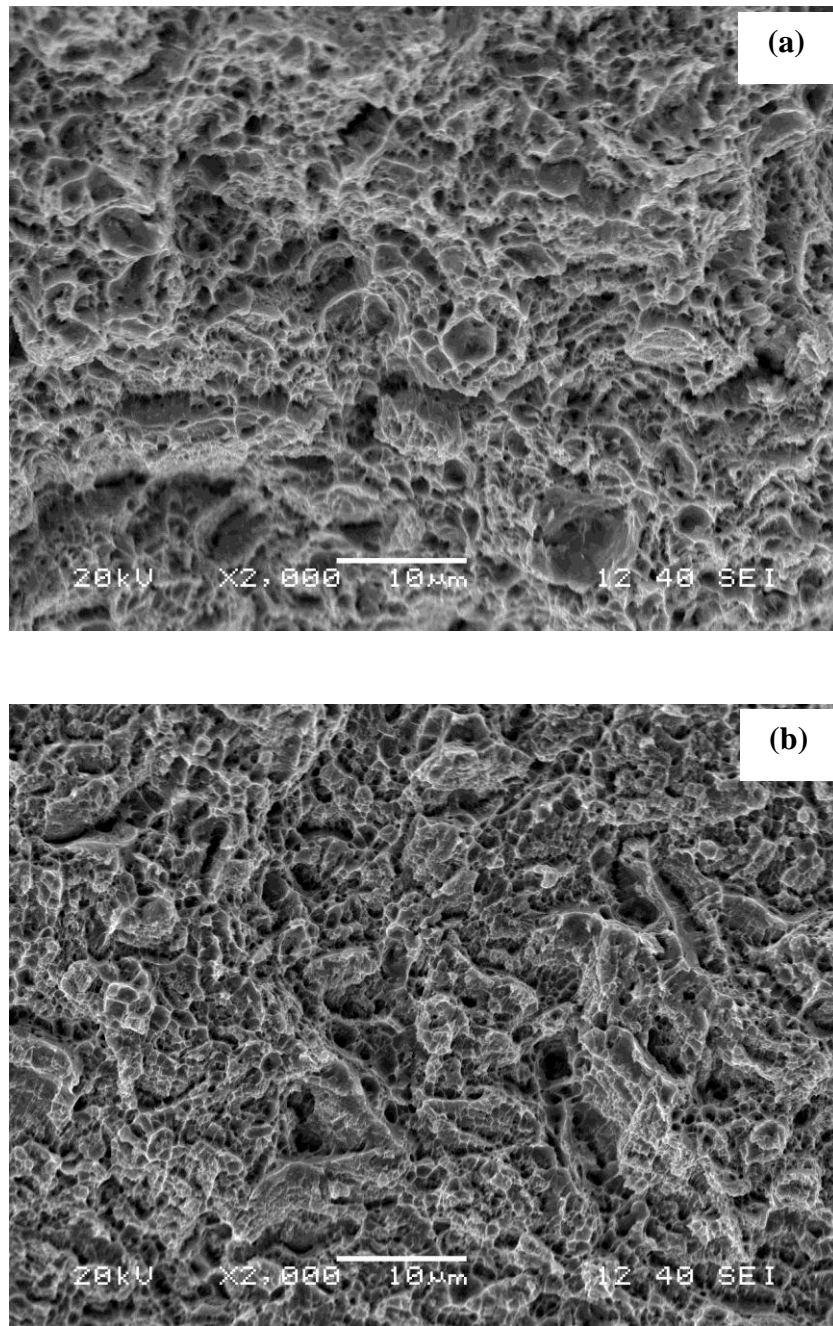


Fig. 4.12: Typical fractographs obtained from the post-ratcheting broken tensile specimens (hardened-tempered) owing to pre-strain levels of (a) 2% and (b) 8%.

Chapter 5

Conclusions

The purpose of this investigation was to study the ratcheting behavior and associated plastic damage of ASTM A668 steel which is potentially used in various engineering sectors like hydro-turbines. Special emphasis was made to understand the effect of pre-strain and pre-corrosion on the ratcheting behavior. The obtained results and their pertinent discussion lead to bring forth the significance of the work towards enhancing the current level of understanding related to ratcheting behavior of the particular steel. This chapter concludes these understandings. In addition, the experience gained from the present work has been used to indicate some of the future directions of research work.

1. Accumulation of ratcheting strain decreases with increase in the level of pre-strain and it is maximum when there is no pre-strain i.e. at 0% pre-strain in normalized and hardened-tempered samples of ASTM class D A668 steel. The decrease in strain accumulation with increasing pre-strain has been explained with formation of dislocations during cyclic loading. The nature of strain accumulation is similar in normalized and hardened-tempered samples; however, the extent is more in normalized samples.
2. Rate of strain accumulation decreases continuously up to about 20 cycles in both normalized and hardened-tempered conditions, but this decrease is much pronounced in initial cycles. A steady state is achieved after 20 cycles, where the strain accumulation is insignificant. It can be stated it acquires a stable dislocation configuration in the substructure of the steel which in turn causes ceasing of strain accumulation.
3. The ratcheting studies on pre-corroded (normalized) specimens indicate that strain accumulation is much more pronounced as that compared with the specimens without corrosion. Most of the pre-corroded samples failed within 100 cycles. This increase in

strain accumulation can be attributed to localized stress concentrations owing to corrosion induced pits.

4. The area under the stress-strain hysteresis loops decrease continuously which indicates that the steel is cyclically hardenable in nature. Results of post-ratcheting tensile tests show that yield strength and ultimate tensile strength values of ratcheted specimens increase as those compared with the unratcheted ones. This fact confirms the steel to be cyclically hardenable.

Scope for future work

The findings of the present study may be expected to add some important database towards designing engineering structures/components using the investigated steel and the outcomes are expected to provide inspiration for further research for better life prediction of structural components subjected to cyclic loading. A number of directions for future research can be suggested from the experience gained in the present work:

- The ratcheting studies on this material can be done using various other test parameters like waveform, stress rate etc. along with studies on substructural variations during the deformation process. Further, tests can be conducted up to failure of a specimen.
- Corrosion tests can be adopted with the ratcheting tests, such that true atmospheric conditions can be implemented.
- Theoretical studies specifically modeling of ratcheting behaviour of materials incorporating substructural features would be an interesting direction of future research. Specifically, attempts should be made to predict fatigue life of materials under asymmetric cyclic loading through models incorporating substructural features.

Bibliography

- [1] G.E. Dieter, *Mechanical Metallurgy*, Third, McGraw-Hill, 2013.
- [2] R.J.Rider, S.J.Harvey, H.D.Chandler, *Int. J. Fatigue* 17 (7) (1995) 507–511.
- [3] Z. Xia, D. Kujawski, F. Ellyin, *Int. J. Fatigue* 18 (1996) 335–341.
- [4] U.C.Ozgen, *Mater. Des.* 29 (2007) 1575–1581.
- [5] M.D. Ruggles, E. Krempl, *J. Mech. Phys. Solids* 38 (1990) 575–585.
- [6] M. Kobayashi, N. Ohno, T. Igari, *Int. J. Plast.* 14 (1998) 355–372.
- [7] Mohamed El May, Thierry Palin-Luc, Nicolas Saintier, Olivier Devos *Int. J. of Fatigue* 47 (2013) 330–339.
- [8] Y. Hirose, T. Mura. *Eng. Fract. Mech.* 22 (5) (1985) 59–70.
- [9] R.W. Hertzberg, (1989), *Deformation and Fracture Mechanics of Engineering Materials*, third edition, John Wiley & Sons, Singapore.
- [10] S. Suresh, (1998), *Fatigue of Materials*, second edition, Cambridge University Press, UK.
- [11] F. Ellyin, (1996) *Fatigue Damage, Crack Growth and Life Prediction*. Springer.
- [12] G. Kang, *Compos. Sci. and Technol.* 66 (2006) 1418–1430.
- [13] F. Yoshida, *Int. J. of Pressure Vessels & Piping*, 44 (1990) 207–223.
- [14] J. W. Ringsberg, *Int. J. Fatigue*, 23(2001) 575–586.
- [15] Q. Gao, G.Z. Kang, and X.J. Yang, (2003), *Theoretical and Applied Fracture Mechanics*, 40 (2003)105–111.

-
- [16] X. Chen, D. Yu, and K. S. Kim, *Mat. Sci. Eng. A* 406 (2005) 86-94.
- [17] T. Hassan, S. Kyriakides (1994), *Int. J. Plasticity*, 10 149-184.
- [18] C. Gaudin, and X. Feaugas, (2004), *Acta. Mater.* Vol. 52 3097–3110.
- [19] D. Kujawski, V. Kallianpur, E. Kremple, *J. Mech. Phys. Solids* 28 (1980) 129–148.
- [20] F. Yoshida, *Int. J. of Pressure Vessels & Piping*, 44 (1990), 207–223.
- [21] F. Yoshida, M. Itoh, E. Shiratori, *Bull. JSME* 24 (1981) 507–514.
- [22] F. Yoshida, S. Yamamoto, M. Itoh, M. Ohmori, *Bull. JSME* 27 (1991) 2100–2106.
- [23] M. B. Ruggles and E. Krempl, *J. Mech. Phys. Solids* 38 (1990) 575–585.
- [24] T. Hassan, S. Kyriakides, *Int. J. Plasticity*, vol. 10 (1994) 149-184.
- [25] Z. Xia, D. Kujwaski and F. Ellyin, *Int. J. Fatigue*, vol. 18 (1996) 335–341.
- [26] M. Kang, Y. Aono, H. Noguchi, *Int. J. Fatigue* 29 (2007) 1855–1862
- [27] S. Paul, S. Sivaprasad, S. Dhar, S. Tarafder, *Mat. Sci. and Eng. A* 528 (2011) 7341– 7349.
- [28] Y. Wang, D. Yu, G. Chen, X. Chen, *Int. J. Fatigue* 52 (2013) 106–113.
- [29] P. De, A. Kundu, P. C. Chakraborti, *Mater. Des.* 57 (2014) 87–97.
- [30] J. Mahato, P. De, A. Sarkara, A. Kundua, *Procedia Eng.* 74 (2014) 368 – 375.
- [31] Y. Chiou, Yi. Jen, W. Weng, *Eng. Fail. Anal.* 18 (2011) 766–775.
- [32] M. Shirinzadeh Dastgiri, J. Mohammadi, Y. Behnamian, A. Eghlimi, A. Mostafaei *Eng. Fail. Anal.* 53 (2015) 78–96.
- [33] L. Weng, Jixi Zhang, S. Kalnaus, M. Feng, Y. Jiang, *Int. J. Fatigue* 48 (2013) 156–164.
- [34] E. Mohamed May, Thierry Palin-Luc, N. Saintier, O. Devos, *Int. J. Fatigue* 47 (2013) 330–339.
- [35] A. Aymen, M. Ahmed, Mansour, M. Wollmann, Lothar Wagner *Surf. Coat. Tech.* 259 (2014) 448–455.

-
- [36] M. Shirinzadeh-Dastgiri, J. Mohammadi, Y. Behnamian, A. Eghlimi, A. Mostafaei *Eng. Fail. Anal.* 53 (2015) 78–96.
- [37] K.Genel, M. Demirkol, T. Gulmez, *Corros. Mater. Sci. Eng.* 88 (2000) 91–100.
- [38] T.Palin-Luc, Pérez-Mora R, Bathias C, G. Domínguez, Paris PC, Arana JL. *Eng. Fract. Mech.*77 (2010) 1953–62.
- [39] F. Oliveira, L. Hernández, J.A. Berrios, C. Villalobos, *Surf. Coat. Tech.*140 (2) (2001) 128–35.
- [40] A. Ragab, H. Alawi, H. Sorein, *Fract. Eng. Mater. Struct.*12 (6) (1989) 469–79.
- [41] P. Nascimento Marcelino, J.C. Voorwald Herman, *Int. J. Fatigue* 32 (2010) 1200–9.
- [42] Y. Hirose, T. Mura, *Eng. Fract. Mech.* 22 (1985) 859–70.
- [43] AJ. McEvily, T. Wei, *Fracture mechanics and corrosion fatigue.* (1972) 381–95.
- [44] W. Zhao, Y.Wang, T. Zhang, Y. Wang, *Corros. Sci.* 57 (2012) 99–103.
- [45] E. Rezig, P.E. Irving, M.J. Robinson, *Procedia Engineering* 2 (2010) 387–396.
- [46] R. Grilli, M.A. Baker, E. James Castle, Barrie Dunn, J. F. Watts, *Corros. Sci.*52 (2010) 2855–2866.
- [47] L. Weng, J. Zhang, S. Kalnaus, M. Feng, Y. Jiang, *Int. J. of Fatigue* 48 (2013) 156–164.
- [48] X. Meng, Zhuoying Lin, F. Wang, *Materials and Design* 51 (2013) 683–687.
- [49] R. Arrabal, B. Mingo, A. Pardo, M. Mohedano, E. Matykina, I. Rodriguez, *Corros. Sci.* 73 (2013) 342–355.
- [50] E 8M-03, ‘Annual Book of ASTM Standards’, Standard test method for tension testing of metallic materials (Metric), 2003, West Conshohocken, PA.
- [51] E606 / E606M-12, Standard Test Method for Strain-Controlled Fatigue Testing, ASTM International, 2012 West Conshohocken, PA.

-
- [52] Avner, Introduction to physical metallurgy, Tata McGraw-Hill Education, 1997.
- [53] V. Raghavan, Physical Metallurgy: Principles and Practice.
- [54] ASM Handbook volume 1 properties and selection irons steels and high permance alloys (1990) 1124-1131.
- [55] G.Z. Kang, Y.G. Li, J. Zhang, Y.F. Sun, Q. Zao, *Theoretical and Applied Fracture Mechanics* 43 (2005) 199-209.
- [56] G. Kang, Y. Liu, Z. Li, *Mat. Sci. and Eng. A* 435–436 (2006) 396–404.
- [57] Y. Liu, G. Kang, Q. Gao, *Int. J. Fatigue* 30 (2008) 1065–1073.
- [58] P. Verma, Ratcheting Fatigue Behaviour and Post-fatigue Tensile Properties of Commercial Aluminium M.tech dissertation submitted in NIT, Rourkela (2011).
- [59] K. Dutta, K.K. Ray, *Mater. Sci. and Eng. A* 575 (2013) 127–135.
- [60] L. Weng, J. Zhang , S.Kalnaus , M. Feng , Y.Jiang, *Int. J. Fatigue* 48 (2013) 156–164.
- [61] Lee EJ. Dependence of strength on corrosion-fatigue resistance of AISI 4130steel. M.S. thesis, Georgia Institute of Technology; 2004.
- [62] K Genel, Demirkol M, T. Gulmez *Mater Sci Eng.* 288 (1) (2000) 91–100.
- [63] T.Palin-Luc, Pérez-Mora R, C.Bathias, G.Domínguez, PC.Paris, JL.Arana, *Eng.Fracture Mech.* 77 (11) (2010) 1953–62.
- [64] F. Oliveira, L. Hernández, JA. Berrios, C. Villalobos, A.Pertuz, ESPuchi-Cabrera, *Surf. Coat Tech.* 140 (2) (2001)128–35.
- [65] A. Ragab, H. Alawi , K. Sorein, *Fatigue Fract. Eng. Mater. Struct.* 1989 12 (6) 469–79.
- [66] P. Nascimento Marcelino, JC. Voorwald Herman, *Int. J. Fatigue* 32 (7) (2010)1–9.
- [67] Y. Hirose, T. Mura, *Eng. Fracture. Mech.* 22(5) (1985) 859–70.
- [68] AJ. McEvily, RP. Wei, *Fracture mechanics andorros. fatigue.* NACE-2; (1972) 381–95.

- [69] R. Ebara, *Mat. Sci. Eng. A* 468–470 (2007) 109–113.
- [70] Y. Wang, X. Chen, D. Yu, G. Chen, *Int. J. Fatigue* 52 (2013) 106–113.
- [71] S. Majumdar and K. K. Ray, *Metallurgical and Materials Transactions A*, 37 (2006) 3541–3553.
- [72] V. Tvergaard, *Journal of Mechanics and Physics of Solids*, 30 (1982) 265–286.
- [73] K. Dutta, Accumulation of ratcheting strain in polycrystalline metallic materials. Ph.D dissertation submitted in IIT Kharagpur (2012).

Dissemination

Conference Presentations

1. S. Tripathy, A. K. Mondal, K. Dutta, (2015) Effect of pre-strain and pre-corrosion on ratcheting behavior of ASTM A668 Class D steel, presented in 5th National Conference on Processing & Characterization of Materials held at NIT Rourkela, Odisha during 12-13 December 2015.

Name Subhrasmita Tripathy
Date of Birth 16.02.1988
Permanent Address Qr.No.D-27/F, Railvihar,
 Chandrasekharpur, Bhubaneswar
E-mail ID subhra359@gmail.com
Languages Known English, Hindi, Oriya
Educational Qualifications:

Year of completion	Course	Institution	Marks Obtained
2010	B.E. (Mechanical Engineering)	Narayan Memorial Institute of Technology Bhubaneswar	7.52
2006	12 th	Jupiter +2 Sc College Bhubaneswar	57 %
2004	10 th	D.A.V. Public School Bhubaneswar	56%